ABSTRACT

ZHANG, XINYU. Receiver Tuning For Wireless Power Transfer Systems. (Under the direction of Dr. Srdjan Lukic).

Inductive, loosely-coupled wireless power transfer system uses resonance between the primary secondary compensation circuits to maximize the power transferred from the transmitter to the receiver output voltage can be regulated using a rectifier and power converter. Resonance is achieved by using compensation circuit containing inductors and capacitors in the receiver side with the same oscillation frequency as the transmitter current frequency. The power transfer efficiency is limited by the coupling condition between the coils and also by detuning (i.e. source or receiver resonance at frequency other than the operating frequency.) Detuning can be caused by transmitter coil current frequency variation, shielding problems and compensation capacitor's non-idealities (such as parasitic resistance, tolerance, aging, temperature, and humidity dependence). Techniques used to eliminate the detuning caused by the above reasons are discussed in detail, suggested solution in literature for active tuning and has been implemented both in simulation and hardware and the results are reported.

This thesis presents an inductive power transfer system with receiver active tuning technique to compensate the tuning condition achieving the power factor correction, maximum power transfer and voltage boost. This is accomplished by using the free-wheeling of inductor current in the tri-state-boost converter working in continuous conduction mode (CCM). The control strategy has been implemented in hardware and simulation. Voltage and power regulation capability was demonstrated for tuned and detuned conditions.

Receiver Tuning For Wireless Power Transfer Systems

by
Xinyu Zhang

A thesis submitted to the Graduate Faculty of
North Carolina State University
in partial fulfillment of the
requirements for the degree of
Master of Science

Electrical Engineering

Raleigh, North Carolina

2014

APPROVED BY:

_____	_____
Dr. Dr. Iqbal Husain	Dr. Alex Q. Huang
	Co-Chair of Advisory Committee

_____

Dr. Srdjan Lukic

Co-Chair of Advisory Committee

BIOGRAPHY

Xinyu Zhang was born on Sep. 5th, 1990 in Sanhe, Hebei Province in People's Republic of China. He received his Bachelor of Engineering degree in Electrical and Electronics Engineering in 2012 from North University of China, Taiyuan, China. He is currently a graduate student at North Carolina State University under the guidance of Dr. Srdjan Lukic. His research interests include power electronics converter and motor control.

ACKNOWLEDGMENTS

I will always remember the days of my master degree when I was 23 in the US. I learned a lot by being a student in the North Carolina State University.

I would like to thank Dr. Lukic for his guidance in this year. I learned a great deal from him in his class and this thesis. I can still feel his wisdom when writing this document now.

I would like to thank Zeljko Pantic. His research in wireless power transfer is really brilliant.

I would like to thank Arvind Govindaraj for answering my questions about power amplifier, circuit and PCB layout.

I would like to thank Kibok Lee for his kindly help in lab.

I would like to thank my family for the support of my study and research.

I would like to thank Fei Xue, Youxi Shao, Xiaoqing Song, Li Wang, Sanzhong Bai, Dr. Xijun Ni, Dr. Ryan Yu, Yang Lei, Haotao Ke, Owais Ahmad, Lloyd Adams, Quadri Oguntade, Jian lv, Jimit Doshi, Nima Yousefpour, Alireza Dayerizadeh, Yuling Zhao, Mingyu Yang, Yang Xu, Yifan Jiang, Rusul Alttaay, Anjie Jiang, Liqi Zhang, Qian Wu, Jingwen Xiong, Xiangqi Zhu, Nan Xue, Shangmin Lin, Qi Tian, Guozhu He, Lin Qu, Yushan Ji. Thank you for your friendship during my master period.

I would like to thank the authors of all the application notes and papers that helped me.

I will always remember the design, the books and papers, the friends, the first job before my 24th birthday.

TABLE OF CONTENTS

LIST OF TABLES

LIST OF FIGURES

1 CHAPTER 1 Introduction

1.1 Background

Wireless power transfer technique has recently been more and more popular. Generally, there are three methods for transfer power wirelessly. The first one is radiative wireless power transfer, also named as far-field when the distance of the power transfer is much greater than the wavelength of the transmitted electromagnetic wave. This is often used in low power scale with far transmission distance. The second one is capacitive power transfer, which uses plate at the transmitter part and receiver part and the air between them as a capacitor achieve the power transmission. The limitation of this method is the maximum value of the electrical field strength because of the air permittivity, so the maximum voltage between the two plates is also limited. The advantages of capacitive power transfer over inductive power transfer are: the electrical field between the plates will not be affected by metal objects nearby and the field leakage is small. The third method is inductive wireless power transfer, which uses magnetic field between the transmitter and receiver to transfer the power. This thesis is mainly focus on inductive power transfer system.

For the inductive power transfer system, the efficiency will be strongly affected by the coupling condition. (See Chapter 2 of this thesis in detail.) Primary coil and secondary coil should be aligned with small distance to increase the coupling coefficient K and receiver coil receives much flux to improve transmission efficiency. Loosely coupled Inductive Power Transfer can work in strongly coupled operation regime when magnetic link potential [1] is big, so increase the operation frequency can improve the coupling situation. But the coil size

and power components switch losses will also increase. Also there is another drawback for loosely couple Inductive Power Transfer system. For a single transmitter to multiple receivers systems, coils of the different receivers will also have influence on each other. The coupled inductance will affects the original receiver compensation network working condition. This is the disadvantage of the inductive method than the capacitive method. Another defect of Inductive Power Transfer (IPT) is foreign metal object placed between the transmitter and receiver will affect the system performance.

The basic structure of IPT is shown in Figure 1-0-1 Typical topology of IPT system. Electrical power can be transferred using the magnetic field between the primary and secondary coils. In the primary side, the power converter is used to provide the power, the primary compensation circuit is a two terminal network, used to compensate the reactance caused by the transmitter coils to lower the VA rating of the switch components or to achieve soft switch. In the secondary side, the receiver coil picks up the power and compensated by the secondary compensation network to reduce the reactive power and to boost voltage. The secondary power converter is used to regulate the voltage.

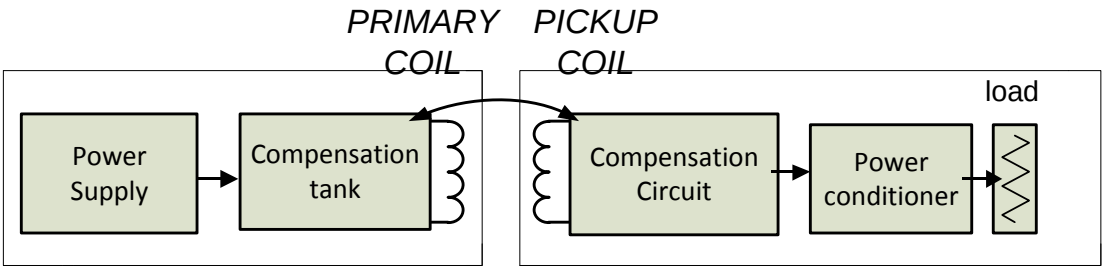

Figure 1-0-1 Typical topology of IPT system

Tuning condition between the secondary compensation circuit LC resonant frequency and the current frequency to maximize the power transferred from the transmitter to the receiver, resulting unity power factor and voltage boost. It is achieved by using compensation circuit containing inductors and capacitors in the receiver side with the same oscillation frequency as the transmitter current frequency. Practically, however, detune will happen. The reasons are: varies of the transmitter current frequency, the non-ideal property of the compensation capacitor such as ESR, tolerance, aging, temperature, and humidity dependence.

1.2 Thesis objective

The aim of this thesis is to present an algorithm for active tuning for the inductive loosely coupled wireless power transfer system in the receiver side. The main feature of this algorithm is its ability to adjust the resonant frequency of the tuning tank to be the same as the current frequency in the transmitter side.

This is accomplished by analyzing the phase of receiver coil voltage in open circuit and working with load situation, using the free-wheeling state of the boost converter inductor current in CCM and the tuning tank together to achieve the power factor correction of the receiver side. The algorithm has been implemented in simulation and on hardware based on PCB and DSP controller.

1.3 Outline

Chapter 2 introduces the basic topology of an inductive power transfer system. The model of compensation circuit based on RLC resonant circuit is developed according to the inductive

power transfer system load modeling. Receiver Structure for wireless power transfer system is analyzed and simulated to show the effect of tuning and compensation.

Chapter 3 consists of the problem of detuning and how to build an active tuning receiver converter. A tri-state-boost converter with control algorithm and compensation circuit using active capacitors tank is presented and simulated in Simulink. In addition, the receiver side Control to output voltage AC small signal model for the receiver with compensation network and rectifier is derived. The differences between normal boost converter, LC filter and the tri-state-converter are analyzed. The differences between PI and hysteresis control are also discussed.

In Chapter 4, the laboratory setup is presented. The PCB layout for the receiver converter, digital controller using TMS320F28335, hardware components and circuit are discussed.

Chapter 5 presents the experiments results.

2 Chapter 2 IPT Receiver Structure

2.1 Introduction

The basic structure of Inductive Power Transfer (IPT) is shown in Figure 1-0-1 Typical topology of IPT system Electrical power can be transferred using the magnetic field between the primary and secondary coils. In the primary side, the power converter is used to provide the power, the primary compensation circuit is a two terminal passive network consist of inductors and capacitors, used to compensate the reactance caused by the transmitter coils to lower the VA rating of the switch components, boost up the voltage, filter out the current or to achieve soft switch. In the secondary side, the receiver coil picks up the power and compensated by the secondary compensation circuit to reduce the reactive power and to boost voltage. The secondary power converter is used to regulate the voltage or actively improve tuning.

Tuning condition between the secondary compensation circuit LC resonant frequency and the current frequency is to reduce the reactive power for the receiver load and get the expected real power, resulting in unity power factor and voltage boost. It is achieved by using compensation circuit containing inductors and capacitors in the receiver side with the same oscillation frequency as the transmitter current frequency. If the load impedance after the tuning tank is resistive, under the perfect tuning condition, the power factor of the receiver is unity which means the receiver converter seen from the pick-up coil is purely resistive. So when putting the receiver close to the transmitter, the transmitter only obtains a purely resistive load which will lead to the minimum reactive power transferred to the secondary

side. In [2] the transmitter topology for the receiver converter test is the LCC compensated to provide constant current in the transmitter track coil branch for the receiver load.

In this chapter, the compensation circuit using two-terminal-network is derived. The basic model for the receiver side pick-up coil, compensation circuit, rectifier and a load resistor is presented.

2.2 RLC resonant circuit

The compensation circuit is composed of inductors and capacitors. With different connection of inductors and capacitors, this two terminal output can be used to match impedance and boost voltage. Properties of the RLC resonant circuits will be used for the compensation circuit design in following chapters.

2.2.1 Series RLC resonant circuit and series compensation

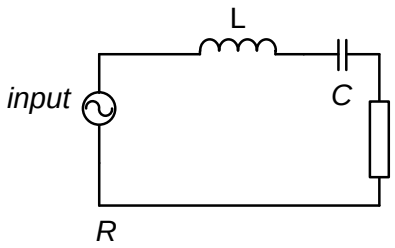

Figure 2-1 series RLC circuit

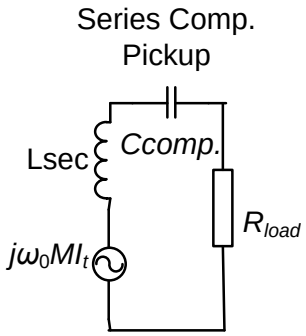

Figure 2-2 series compensation for receiver

Figure 2-1 series RLC circuitshows the basic RLC resonant circuit. Resonant frequency is $\omega_0 = \frac{1}{\sqrt{LC}}$, with quality factor

$$Q_{series} = \frac{1}{\omega_0 RC} = \frac{\omega_0 L}{R} \quad [2.1]$$

When the input voltage frequency equals the resonant frequency, input impedance is R with the output voltage the same as input voltage.

For IPT system compensation circuit, series compensation for the transmitter or receiver coil inductance is similar to the RLC series resonant circuit in Figure 2-2 series compensation for receiver. M is the mutual inductance between the primary and pick-up coils L, $C_{comp.}$ is the compensation capacitor. Frequency of the input equals resonant frequency ω_0. This compensation will help reflected the receiver load to transmitter track branch as purely a resistor to reduce reactive power.

2.1.2 Parallel resonant circuit, low pass filter and parallel compensation

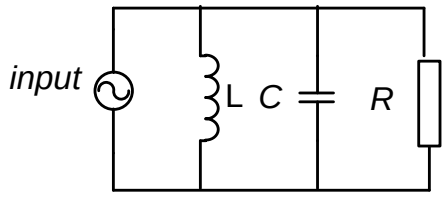

Figure 2-3 parallel resonant RLC circuit

Figure 2-3 parallel resonant RLC circuit shows a basic parallel resonant circuit with resonant frequency$\omega_0 = \frac{1}{\sqrt{LC}}$, quality factor

$$Q_{paral} = \frac{R}{\omega_{0L}} = \omega_0 RC = R\sqrt{\frac{C}{L}} \quad [2.2]$$

Figure 2-4 low pass filter shows a low pass filter which is very similar to the parallel compensation circuit topology.

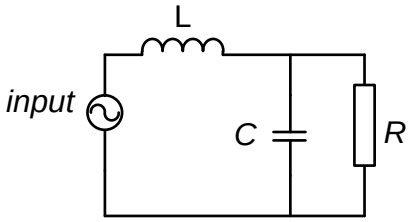

Figure 2-4 low pass filter

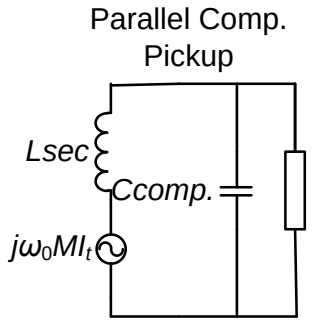

Figure 2-5 parallel compensation circuit

Network like Figure 2-4 low pass filteris a low pass filter. When the input AC frequency w is the same as the resonant frequencyω_0, then a simple voltage calculation shows that output voltage value is:

$$\mathrm{V_{out}} = Q_{paral} V_{input} = R\sqrt{\frac{C}{L}} V_{input} \text{ [2.3]}$$

which means that the current through load R is

$$\mathrm{I_{load}} = V_{input}\sqrt{\frac{C}{L}} \text{ [2.4]}$$

When the input voltage is constant, the current through that branch is constant. This topology can be used in transmitter compensation circuit design because of the constant current property, system resistive load put in the load branch. When the track current$\mathrm{I_s}$ is constant, the receiver pick-up voltage

$$\mathrm{V_{picupk}} = MI_s \text{ [2.5]}$$

only changes with mutual inductance M. This makes the system easier to analysis.

For the receiver compensation circuit, advantages of parallel compensation over series one also include the voltage boost and start up current limit. During the star up process when the voltage is small, the load current won't be too big. In addition, a high Q of the parallel compensation can boost up the output voltage.

2.3 Inductive Power Transfer System Load Modeling

2.1.1 Basic Transmitter Structure

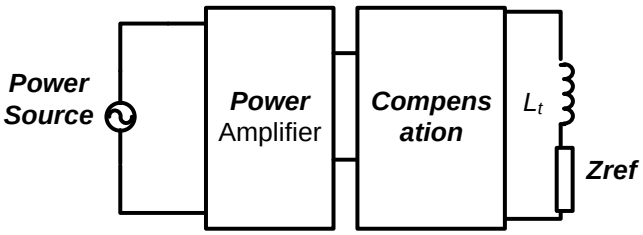

Figure 2-6 basic transmitter model

The basic model of the transmitter is shown in Figure 2-6 basic transmitter . The transmitter side is essentially a power amplifier (or inverter) with an impedance matching circuit. The impedance matching circuit is also a passive network consists of inductors and capacitors, like the receiver side. The transmitter side needs the compensation to improve the power regulation, voltage boost and filter effect at the output of the inverter.

Transmitter is used to generate AC voltage to power up the receiver, compensation circuit at the output of the full-bridge is used to compensate the reactance, voltage boost and filter the current through the coil to an expected pure sine wave. Imagine all the components are ideal at this step. The inductor Lt in the picture is the transmitter coil inductance. Z_{ref} represents the load of the secondary side reflected value in the transmitter coil branch. If the transmitter coil current is I_t, then the receiver obtains power

$$P_{receiv} = {I_t}^2 Z_{ref} \quad [2.6]$$

The previous session discussing RLC low pass filter property introduced a method to provide constant current in a branch. Reference [5] recommends a LCC compensation for the primary coil after the voltage source inverter:

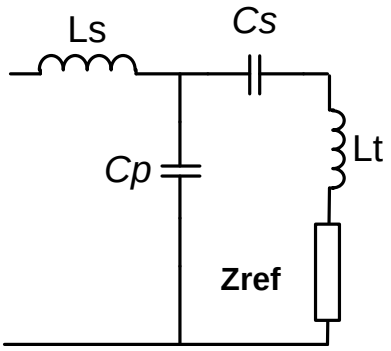

Figure 2-7 recommended compensation for transmitter coil L_t

L_s is series inductor, C_p is parallel capacitor, when they are tuned under the input frequency and the other branch is purely resistive, then current (only consider the first harmonic)

through that branch is constant. Then series capacitorC_p is used to series compensate the coil inductance with a purely resistive receiver reflected load. The inverter output voltage first harmonic peak value $V_{inv,1} = \frac{4V_{dc}D}{\pi}$. The transmitter coil branch current: $I_t = V_{inv,1}\sqrt{\frac{C_p}{L_s}}$. So $C_p = \frac{I_t}{\omega_0^2 C_p}$ and $L_s = \frac{1}{\omega_0^2 C_p}$. When C_s value is $C_s = \frac{C_p}{L_t/L_s - 1}$, then the first harmonic of the transmitter coil voltage and current are in phase with each other.[5]

Reflected receiver load Z_{ref} can be compensated by the receiver circuit to be resistive to reduce reactive power.

The basic topology and compensation of the receiver is shown in Figure 2-8 basic topology of receiver and Figure 2-9 receiver parallel compensation. Where inductor L_{sec} means the pick-up coil, $C_{comp.}$ represents the compensation capacitor with Z_r the receiver load impedance. Figure 2-9 receiver parallel compensation shows the receiver pick up model. Voltage V_{oc} is the open circuit voltage of the pick-up coil, L_{sec} is the self-inductance. $V_{oc} = MI_t\omega$

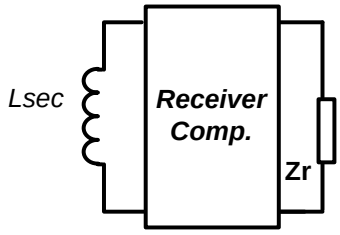

Figure 2-8 basic topology of receiver

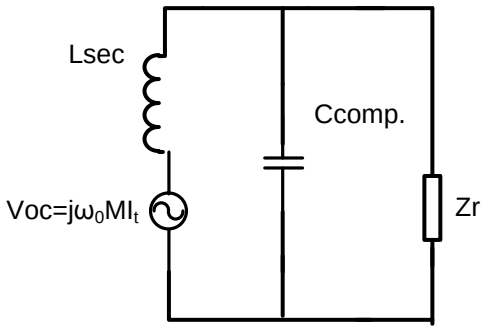

Figure 2-9 receiver parallel compensation

where M is the mutual inductance between the primary coil and the pick-up coil, I_t is the current through the primary coil inductor and ω the radian frequency of the current I_t.

2.1.2 load modelling of the receiver

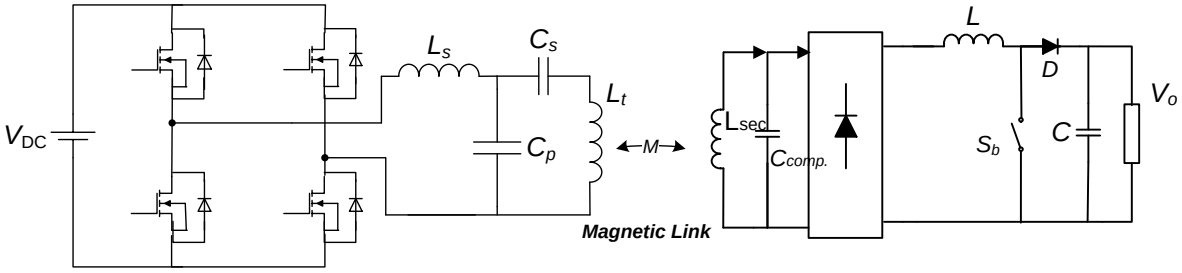

Figure 2-10 Parallel compensated boost converter receiver IPT system

Take parallel compensation receiver for example to determine the reflected impedance value in the primary side: when the input electrical frequency equals this resonant frequency, tuning condition works. In the smith chart plot, the RLC network reflected impedance seen from the input side of the network is purely resistive. The reflected impedance Z_{ref} is in series with the transmitter self-inductance L_t as shown in Figure 2-9 receiver parallel compensation

Under the tuning condition, real power of the secondary side all goes to the load Z_r (resistive) under the resister voltage

$$V_{Zr} = \sqrt{\frac{Ccomp.}{Lsec}}\, ZrV_{oc} \quad [2.7]$$

Voltage $V_{Zr}$is in proportional with the parallel resister value Z_r, and current flows through that resister branch is constant with the value of $\sqrt{\frac{Ccomp.}{Lsec}}\, V_{oc}$. So, when the resister branch is open circuited, which means the value of the load resister is infinity, voltage of the capacitor ideally is also infinity. The equivalent input load impedance Z_{in} seen from the controllable voltage source V_{oc} can be derived using the real power:

$$Z_{in} = \frac{Lsec}{RCcomp.} [2.8]$$

In Figure 2-11 input load impedance Z_{in} seen from V_{oc}shows the Z_{in}.

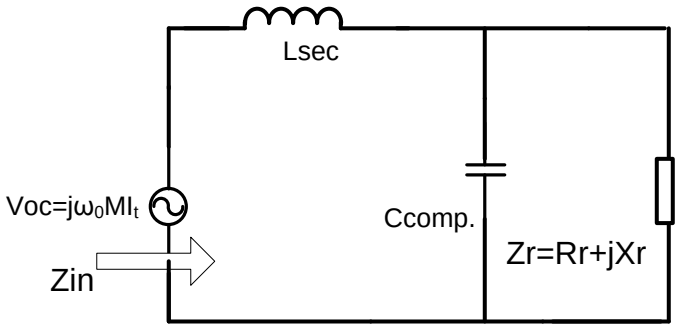

Figure 2-11 input load impedance Z_{in} seen from V_{oc}

The picked up open circuit voltage is $V_{oc} = MI_s\omega$. Using the power relation, value of Z_{ref} in the transmitter branch can be obtained:

$$Z_{ref} = \frac{M^2 R}{Lsec^2} \text{ [2.8]}$$

Also, the power delivered to the pick-up side can be written in an equivalent form:

$$P_{pickup} = Q_{po}\, I_{sc}\, V_{oc} \text{ [2.9]}$$

$$I_{sc} = \frac{V_{oc}}{\omega_s L_{sec}} = \frac{I_s M}{L_{sec}} \text{ [2.10]}$$

Parallel compensation is preferred to series because of its ability to boost voltage.

where I_{sc} represents the short circuit current of the pick-up coil. Define reflected impedance in the transmitter coil branch as

$$\mathrm{Z_{ref}} = \mathrm{R_{load}} + \mathrm{jX_{load}} = \frac{M^2\omega^2}{Z_{in}} \text{ [2.11]}$$

Table 2.3-1 receiver impedance reflected to the primary coil branch

	Parallel compensation	Series compensation
Reflected resistance R_{load}	$R_{load\_0}\frac{(\omega^*)^2}{((\omega^*)^2-1)^2Q^2+(\omega^*)^2}$	$R_{load\_0}\frac{(\omega^*)^4}{((\omega^*)^2-1)^2Q^2+(\omega^*)^2}$
Reflected reactance X_{load}	$R_{load\_0}\frac{-(\omega^*)^3\left[\frac{(\omega^*Q)^2-Q^2+1}{Q}\right]}{((\omega^*)^2-1)^2Q^2+(\omega^*)^2}$	$R_{load\_0}\frac{-(\omega^*)^3((\omega^*)^2-1)Q}{((\omega^*)^2-1)^2Q^2+(\omega^*)^2}$
Receiver Quality factor Q	$L_{se}\omega_0 R_r\frac{R_r}{\omega_0 L_{sec}}$	$\frac{\omega_0 L_{sec}}{R_r}$
R_{load_0} (tuning)	$\frac{M^2}{{L_{sec}}^2}R_L$	$\frac{{\omega_0}^2M^2}{R_r}$

In the same way, the reflected impedance value in different frequencies and different compensation circuits are derived and shown in Table 2.3-1 receiver impedance reflected to the primary coil branch according to reference [1].

2.4 Inductive Power Transfer Receiver Structure

2.1.3 Bridge Rectifier

Reference article [4] states that the rectifier in the receiver side with AC voltage source and resonant tank can be transformed into the equivalent DC model when the receiver is perfectly tuned and the rectifier diodes' current are continuous. With a very large filter inductor after the rectifier, Fourier analysis can be used to transform the rectifier to an ideal transformer.

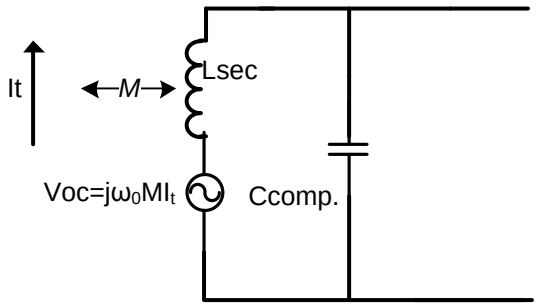

Figure 2-12 parallel compensated pick up side

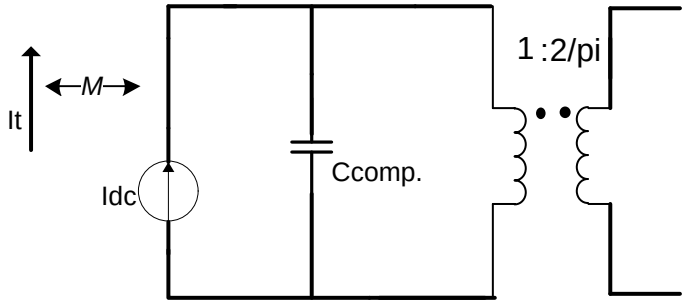

Figure 2-13 parallel compensated pick up side with rectifier

The equivalent DC model input DC current

$$I_{dc} = \frac{I_{sc}}{\sqrt{2}} = \frac{M\, I_s}{\sqrt{2}\, L_{sec}} \text{ [2.12]}$$

where I_{sc} is the equivalent short circuit current of pick-up coil.

In the above equation, receiver pick up coil short circuit current I_{sc} and transmitter coil current I_s are in their RMS value. The resulting transformer equivalent turn ratio with input in AC is $N_{AC} = 1{:}\frac{2\sqrt{2}}{\pi}$, and the equivalent turn ratio in the DC model $N_{DC} = 1{:}\frac{2}{\pi}$ [4].

However, in the chapter 3 with the tri-state-boost converter after the rectifier, the input current of the rectifier is discontinuous. The detail model of the rectifier with tri-state-boost converter will be derived in the following chapter.

Normally, the receiver output voltage needs to be regulated, so in most cases there is a converter after the rectifier. For the basic buck or boost topology: Because the compensation circuit is determined to be parallel for the benefit of voltage boost function and current ratio property of the load branch over series compensation, the power converter input current of buck converter is discontinuous which needs an additional input filter. So boost topology converter is chosen here for the power flow control.

2.1.4 Boost converter

For a conventional boost converter placed after the rectifier at the receiver side, R_L is load resister, D_b the switch duty cycle. Take steady state analysis of the boost converter can get the input load of the converter is $(1 - D_b)^2 R_L$.

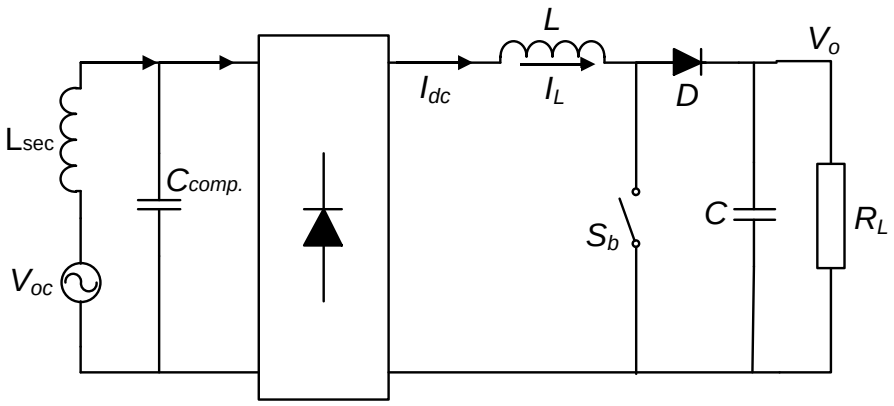

Figure 2-14 parallel compensated boost converter receiver

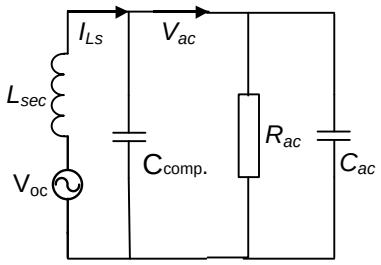

Figure 2-15 principle of injected impedance

In Figure 2-15 principle of injected impedance the R_{ac} and C_{ac} are the injected resister load and capacitor by the following power conditioner. For the boost converter combined with the transformer model discussed previously shown in Figure 2-15 principle of injected impedance,

$$R_{ac} = \frac{\pi^2}{8}(1 - D_b)^2 R_L \quad [2.13]$$

Assuming that the inductance in Figure 2-15 principle of injected impedance is very large and the input current of the rectifier is continuous. When boost converter switch duty cycle D_b is 0, working as a filter, then R_{ac} value is:

$$R_{ac} = \frac{\pi^2}{8} R_L \quad [2.14]$$

Conventional boost converter with parallel compensation in the receiver side model is derived in reference [4].

$$\frac{\widehat{V_o}}{\widehat{I_t}} = \frac{(\frac{2}{\pi})\frac{M}{\sqrt{2}L_2}(1-D)}{LC_{comp.}CS^3+\left(C_{comp.}Cr_L+\frac{LC_{comp.}}{R_L}\right)S^2+\left(C_{comp.}(1-D)^2+\left(\frac{2}{\pi}\right)^2 C+\left(\frac{2}{\pi}\right)^2\frac{C_{comp.}r_L}{R}\right)S+\left(\frac{2}{\pi}\right)^2\frac{1}{R_L}} \quad [2.15]$$

$$\frac{\widehat{V_o}}{\hat{d}} = \frac{-\left(\frac{2}{\pi}\right)\frac{M}{\sqrt{2}L_{sec}}I_t\left[\left(\frac{2}{\pi}\right)^2 LC_{comp.}S^2+\left(\frac{2}{\pi}\right)^2\left(\frac{r_L}{L}-(1-D)^2\frac{R_L}{L}\right)LC_{comp.}S+1\right]}{LC_{comp.}CS^3+\left(C_{comp.}Cr_L+\frac{LC_{comp.}}{R_L}\right)S^2+\left(C_{comp.}(1-D)^2+\left(\frac{2}{\pi}\right)^2 C+\left(\frac{2}{\pi}\right)^2\frac{C_{comp.}r_L}{R_L}\right)S+\left(\frac{2}{\pi}\right)^2\frac{1}{R_L}} \quad [2.16]$$

The third order control to output transfer function is the model for the parallel compensated boost converter receiver. Although there are two RHP zeros there which need to be considered when designing fast controller , the model has one dominent real pole [4].

In the above equations, M means the mutual inductance between the primary and secondary coil. L,C and R_L are the inductance, capacitance and load resistance shown in Figure 2-14 parallel compensated boost converter receiver. r_L means the DCR of the boost inductor. Hysteresis control of a normal buck converter in CCM is forever stable for any choice of system parameters and so is the case with normal DC-DC boost converters under constant input voltage according to [8]. The simulation result and hardware setup will be discussed in the following chapters.

The high order model of the IPT system leads to a complecated traditional controller design. Since the boost converter in CCM is always stable in output voltage mode hysteresis control, the output voltage bang-bang control is used here so simlicity and robustness. Also, the switching frequency can be lower without considering its influence to linear controller cutoff frequency and this leads to less EMI problem.

2.5 System Summary of Inductive Power Transfer Model

2.1.5 Transmitter simulation

According to [2], the transmitter compensated by a LCC network working in Zero Phase Angle (ZPA) mode is shown in Figure 2-16 transmitter topology as discussed in previous session 2.1.2.

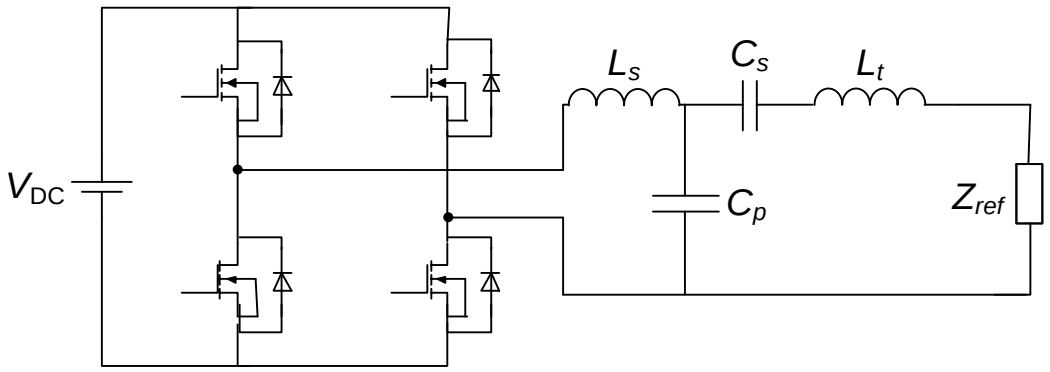

Figure 2-16 transmitter topology

In simulation all the parameters and values are shown in Table 2.5-1 transmitter parameters:

Table 2.5-1 transmitter parameters

Model Parameter	Symbol	Value	Unit
Series Compensation Inductor	L_s	10	μH
Parallel Compensation Capacitor	C_p	253.3	nF
Series compensation Capacitor	C_s	105.4	nF
Transmitter Coil Self Inductance	L_t	24.03	μH
Input DC Voltage	V_{dc}	5	V
Duty Cycle of Full bridge	D	80%	1
Reflected Receiver load	Z_{ref}	15	Ω

Simulation Result:

Transmitter coil branch current plot in simulation:

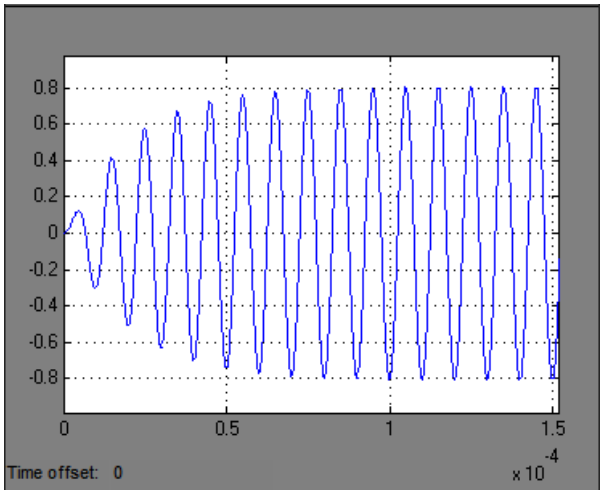

Figure 2-17 transmitter coil current

Transmitter coil voltage:

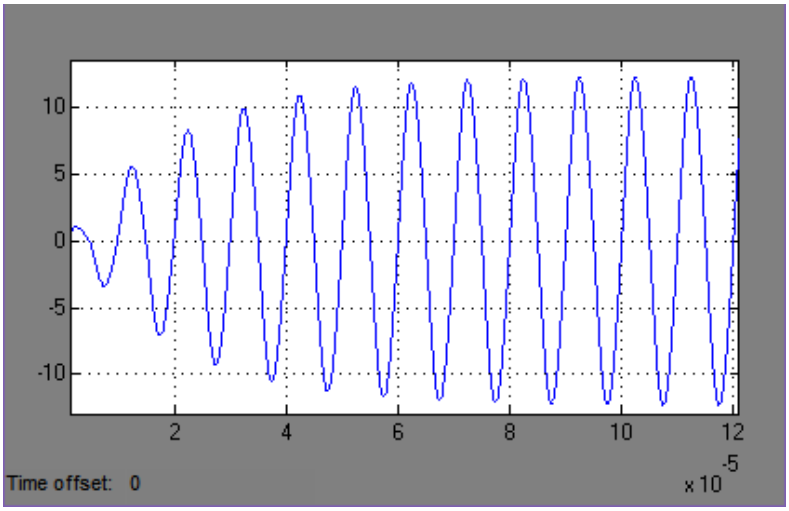

Figure 2-18 transmitter coil voltage

In Table 2.5-1 transmitter parameters2, all the simulation results match the design in previously discussed method using the parallel compensation and series compensation properties. For instance, the calculation result of I_t maximum peak value is 0.816A, the same as the simulation. The inverter output voltage first harmonic peak value $V_{inv,1} = \frac{4V_{dc}D}{\pi}$, and the first harmonic voltage peak value is 5.01V. Current I_t is defined by the parallel compensation tank. Series compensation is used to compensate the transmitter coils reactance. The electrical models in Simulink simulation are ideal models which are very helpful for components selection. In Chapter 4, components of both transmitters and receivers are selected, with better transient model simulated in PSpice and hardware test.

Table 2.5-2 transmitter simulation results

Results Parameters	Symbol	Value (AC Peak)	Unit
Series Inductor Current	I_{Ls}	2.03	A
Parallel Capacitor Voltage	V_{cp}	12.2	V
Series Capacitor Voltage	V_{cs}	12.23	V
Transmitter Coil Voltage	V_{Lt}	12.23	V
Transmitter Coil Current	I_t	0.816	A
Series Inductor Current	$I_{Lseries}$	2.026	A

2.1.6 Receiver simulation summary

1 parallel pick up compensate simulation

With only a parallel compensation capacitor and a load resistor, receiver under tuning condition should obtain AC voltage across the load resister with the value

$$\mathrm{V_o} = \sqrt{\frac{C_{comp.}}{L_{sec}}} R V_{oc} \quad [2.17]$$

as discussed above. Then it also should be equivalent to a load of

$$Z_{in} = \frac{L_{sec}}{R C_{comp.}} \quad [2.18]$$

generating the same load power. $Q = \sqrt{\frac{C_{comp}}{L_{sec}}} R = 3.41,$ The expected output voltage peak value is 3.41V.

Table 2.5-3 basic receiver components parameters

Parameter	Symbol	Value	Unit
Pick-up Coil Open Circuit Voltage	$\mathrm{V_{oc}}$	1 (AC Peak)	V
Secondary Coil self-inductance	$\mathrm{L_{sec}}$	23.8	μH
Compensation Capacitance	$\mathrm{C_{comp.}}$	106.43	nF
Load Resistance	R	51	Ω

With the simulation parameter shown in Figure 2-18 transmitter coil voltage the output voltage peak value is about 3.41V, which is the same as expected. With the same simulation parameters shown above, place a diode bridge between the compensation circuit and load resister R, the resulting voltage across compensation capacitor AC maximum value should be the same, as shown in Figure 2-19 voltage across compensation capacitor with only resistor load case.

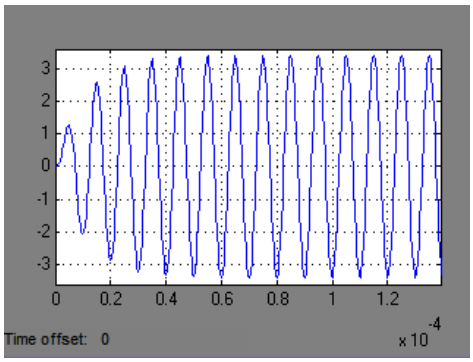

Figure 2-19 voltage across compensation capacitor with only resistor load case

Sometimes simulation results will not meet the expected value, that's caused by the non-ideal property of diodes such as snubber parameters by affecting the tuning situation. Practically, fast recovery diode should be used here or the final wireless power transfer efficiency will be greatly reduced.

With the same simulation parameters shown above, place a diode bridge and a LC filter with load resister R_L.

Table 2.5-4 receiver boost converter parameters

Parameter	Symbol	Value	Unit
Inductance	L	120	μH
Capacitor	C	44	μF
Boost Load Resistance	R_L	51	Ω

The inductor current should be always continuous to make sure the diode bridge model derived in reference article [4] works fine. Result of this simulation meets the diode bridge calculation. So the circuit quality factor is$\frac{\pi^2}{8}$ timers bigger than the previous case

$$V_{ac} = V_{dc}\frac{\pi}{2} (V_{ac} \text{ in AC peak value}) \quad [2.19]$$

Table 2.5-5 simulation results of boost converter receiver V_{ac} and V_{out}

Parameter	Symbol	Value	Unit
Resonant tank voltage	V_{ac}	4.265	V
Output voltage	V_{out}	2.687	V

Inductor of the DC part circuit should be large enough to make sure the DC side current is continuous. As long as the inductance is large enough, ideally no matter how big the value of inductance and capacitance won't affect the mean value of the load resister voltage. As previously discussed, R_{ac} in this case is $\frac{\pi^2}{8}R_L$ according to the diode bridge model. The simulation result equals the expected value. The finish of the start-up process is that the inductor current becomes a steady value: I_{steady}.

$$I_{steady} = \sqrt{\frac{C_{comp.}}{L_{sec}}} \quad [2.20]$$

the limitation current of parallel compensation topology.

Parallel compensated boost converter Receiver

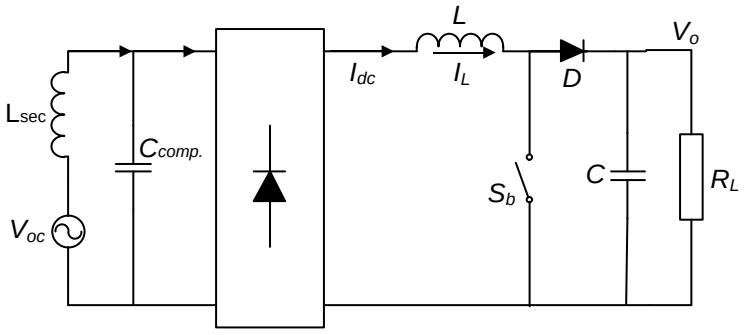

Figure 2-20 parallel compensated boost converter receiver

As shown in figure 2.5.5, all the simulation parameters are shown in Table 2.5-6 boost converter receiver simulation parameters

Table 2.5-6 boost converter receiver simulation parameters

Parameter	Symbol	Value	Unit
Pick-up Coil Open Circuit Voltage	V_{oc}	6 (AC Peak)	V
Secondary Coil self-inductance	L_{sec}	23.8	μH
Compensation Capacitance	$C_{comp.}$	106.43	nF
Boost Converter Inductance	L	120	μH
Boost Converter Capacitor	C	44	μF
Boost Load Resistance	R_L	50	Ω
Hysteresis Control Band	4.9 ~ 5		V

Receiver Output Voltage plot is shown in figure 2.5.6 and figure 2.5.7

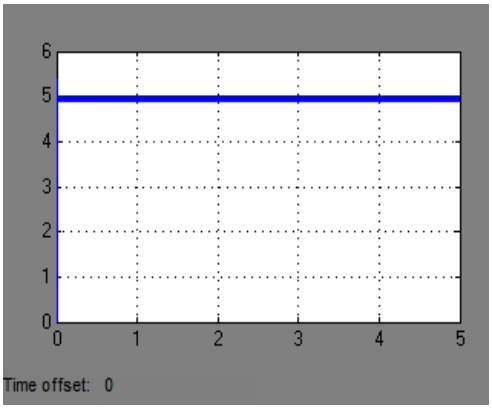

Figure 2-21 output waveform of boost converter receiver

Results of the receiver boost converter are listed in Table 2.5-7 results of the receiver boost converter

Table 2.5-7 results of the receiver boost converter

Parameter	Symbol	Value	Unit
Switching Frequency	f_s	17.3	Khz
Output voltage rise up time	t_r	8.93	μs
Output voltage drop time	t_d	48.8	μs
Maximum Inductor Current (steady state)	$I_{L,max}$	0.875	A
Minimum Inductor Current	$I_{L,min}$	0.24	A

In this situation, boost converter still working in CCM with about 17.3Khz switching frequency hysteresis controlled to maintain the output. Chapter 4 will discuss more details about this.

Waveforms of V_{oc}, control D_b and inductor current in matlab simulation is shown in Figure 2-23 boost converter input voltage, control signal, I_L and V_{out} waveforms with output capacitance $120\mu F$in a same time scale.

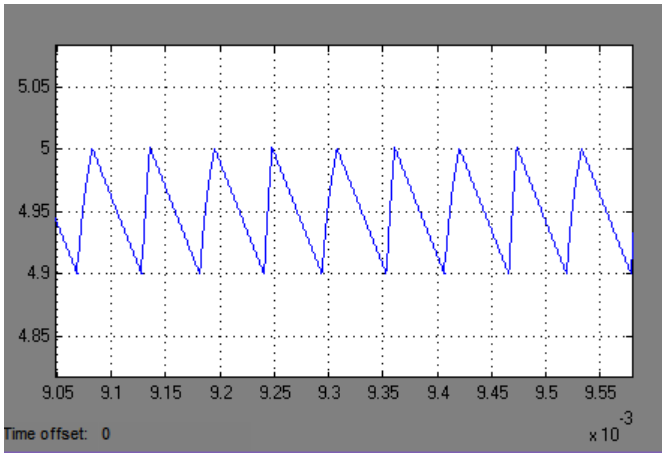

Figure 2-22 zoom-in of figure 2.5.6

During the start-up of the boost converter in output voltage hysteresis control, output voltage is still less than the up limit of the hysteresis window, control switch S_b is off, and the receiver is working like a parallel compensated filter.

When hysteresis window top value is less than the nominal filter output voltage, the controller can work. To make sure the filter inductor DC current is continuous, inductance value still need to be large. At this short time receiver is working as a filer. Then the hysteresis band top limit has been triggered by the output voltage, switch S_b is controlled on.

When boost switch S_b is on, only L is connected with the rectifier. Ideally it is a second order system until the current through inductor L changes direction. V_{ac} at the other side of the rectifier will help the inductor current increase until V_{ac} is zero. This is because the reflected resistor is 0, circuit steady state quality factor is 0. When boost switch is off, then it is like a filter in that short time, output voltage will rise like the filter discussed. The filter voltage at

V_{ac} side needs to consider the harmonics until the output voltage gets the hysteresis band up limit. Because of the inductance is very large, the current waveform high order harmonic is filtered out. In addition, the boost control frequency will increase with a smaller ripple output voltage, like shown in Figure 2-23 boost converter input voltage, control signal, I_L and V_{out} waveforms with output capacitance $120\mu F$, only increase the output capacitance to $120\mu F$ without changing any other parameters.

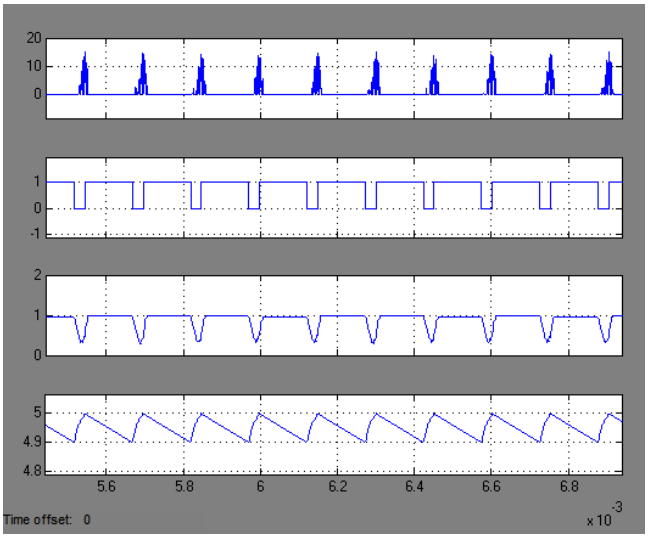

Figure 2-23 boost converter input voltage, control signal, I_L and V_{out} waveforms with output capacitance $120\mu F$

When changing the inductance value to 400μH, waveforms are shown in Figure 2-24 boost converter input voltage, control signal, I_L and V_{out} waveforms when inductance is 400μH.

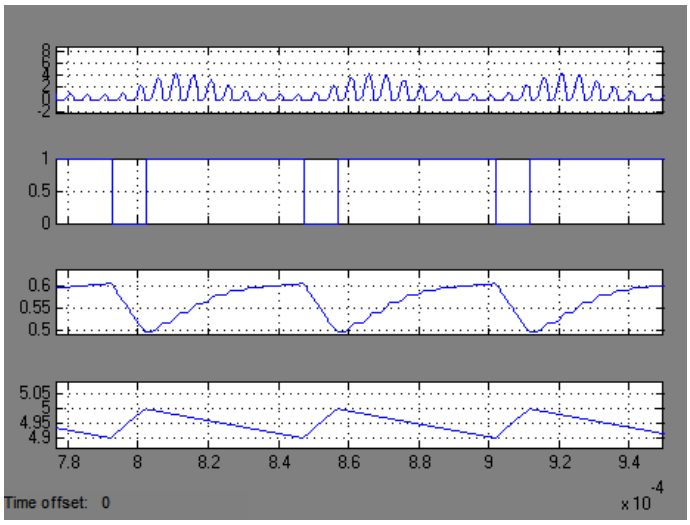

Figure 2-24 boost converter input voltage, control signal, I_L and V_{out} waveforms when inductance is 400μH

The dc side inductor L_{dc} value should be large enough to make the system run into CCM, or the output voltage will not be constraint in the hysteresis band. Switching frequency can be defined by the equivalent filer case input voltage V_{ac}, boost converter side L and C. The converter switches S_b to change the equivalent R_{ac} dynamically to change the input voltage.

$$V_{in} = (1 - D_b)V_{out} = R_{ac}\sqrt{\frac{C_{comp.}}{L_{sec}}}\,V_{oc} = \frac{\pi^2}{8}(1 - D_b)^2 R_L\sqrt{\frac{C_{comp.}}{L_{sec}}}V_{oc} \quad [2.21]$$

When switch S_b is on, it not only cut the line between V_{in} and V_{out} in circuit but also reduce V_{in} to 0 because of the resonant circuit property. Then, value of D_b is determined by V_{out}, R_L and V_{oc} as shown in equation[1.21].

$$D_b = 1 - \frac{V_{out}}{V_{oc}} \frac{8}{\pi^2 R_L} \quad [2.22]$$

Switching frequency is determined by L and C. A very interesting performance of the receiver converter is: when switching frequency is much lower than the frequency of input V_{oc}, the R_{ac} and V_{in} change from V_{oc} is not an equivalent value in dynamic process but a value sometimes is 0 and sometime is other value. When D_b is on then voltage V_{ac} will drop to 0, when switch is off V_{ac} will increase. When switching frequency is chosen to be very high, then V_{ac} waveform is overall continuous but within one period the waveform is not necessarily a standard sine wave.

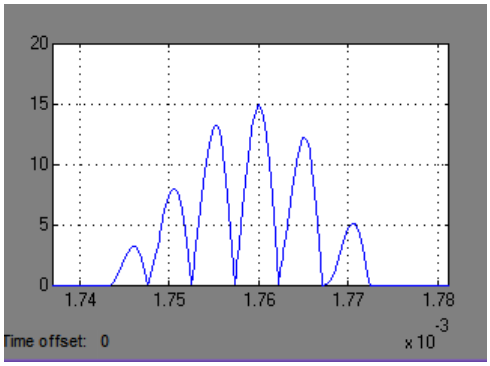

Figure 2-25 V_{ac} after rectifier waveform in 12Khz switching frequency case

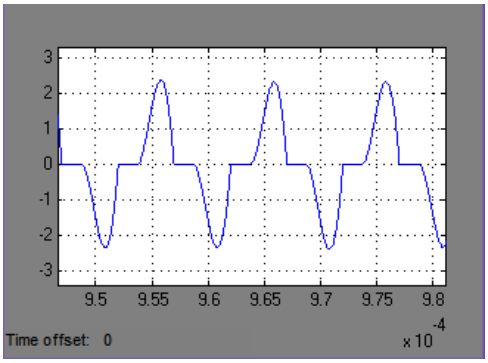

Figure 2-26 V_{ac} waveform in 250Khz switching frequency case

Normally buck converter is easy to use voltage type hysteresis control, because of the input current and output voltage being in phase with each other. While for a normal boost converter alone, output capacitor voltage and inductor current are not. Boost converter hysteresis control can work with DC input voltage higher than the output voltage, but the inductor current will keep increasing.

For boost converter parallel compensated at receiver, output voltage goes up during the switch off period, inductor current will drop from parallel compensation topology current limitation: I_{steady}. And it is very important that the inductance L should be large enough so current is continuous and the voltage control bang up limit should be smaller than the filter voltage output.

In Figure 2-25 V_{ac} after rectifier waveform in 12Khz switching frequency case and Figure 2-26 V_{ac} waveform in 250Khz switching frequency case, during the switch S_b turn on and turn off period, the waveform of input voltage has some transient process because of the boost converter inductance.

3 Chapter 3 Active Tuning Receiver Converter

3.1 Introduction

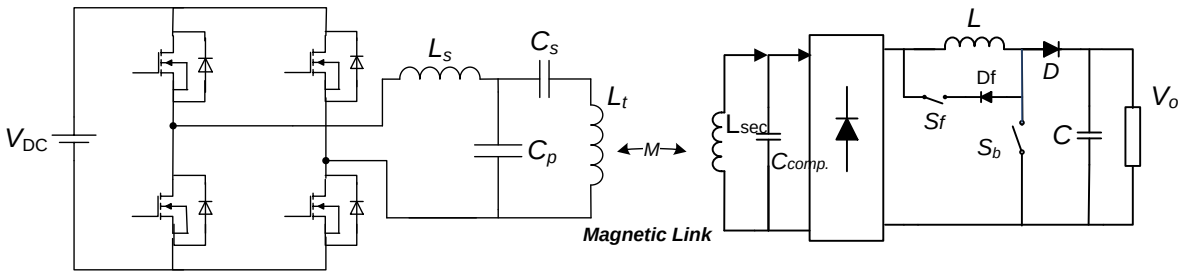

Figure 3-1 Parallel compensated tri-state-boost receiver IPT system

This chapter presents the problem of detuning and how to build an active tuning receiver converter. A tri-state-boost converter with control algorithm and compensation circuit using active capacitors tank is presented and simulated in Simulink. In addition, the receiver side control to output voltage AC small signal model for the receiver with compensation network and rectifier is derived. The differences between normal boost converter, LC filter and the tri-state-converter are analyzed. The differences between PI and hysteresis control are also discussed.

In chapter 2, the output of the resonant tank goes to the rectifier with boost converter to achieve output voltage regulation. For reactive power control: the inductive coupled power transfer system in the previous chapter topology actually will not be ideally under tuning

condition. There are some reasons for that. The transmitter power source frequency may have slight error when it is under open circuit control. The other possible reason for the detuning is the variation of the receiver side components' value. For example, some capacitor has big equivalent series resistance (ESR) which will affect the ideal compensation effects, some capacitor's value changes greatly with temperature and other environmental parameters like humidity. So a careful chosen of the capacitor in material and package is needed. Some capacitors have very big manufacturing tolerance value, and some capacitor value changes with time.

Besides the above two reasons, the shielding of transmitter coil and receiver coils is very important. A metal object locating between the system coils resulting in the decrease of the mutual coupling, or a foreign object locating behind the receiver coil only influencing the self-inductance value of the pick-up inductor can cause the poor shielding problem[1]. Induced eddy current in a conductive object always causes a reduction of the pick-up self-inductance, thus bringing resonant tank detuning issues.

As a result, detuning of the ideal parallel compensation needs to be taken into consideration in reality. [2]

The goal is to design a power converter at the receiver side to tune the compensation network. And as a result the input reactance of the rectifier with the power converter can help the parallel compensation tank to achieve real time active perfect tuning. The mark of perfect tuning is the input impedance of the receiver is purely resistive. As shown in the topology in Figure 2-15 principle of injected impedance, when the load after the resonant tank is a resistor for easy analysis, resonant tank inductor and capacitor are already perfectly tuned,

the reactance of power converter injected reactance should be zero, or it will affect the tuning of the resonant tank. And the input Z_{in} in this case is also resistive. So voltage measured across the inductor and capacitors are in phase with the current through the resister.

Reference [2] proved that tri-state-boost can actively tune the circuit even when detuning happens which is another advantage over standard boost converter. Chapter 2 simulates the boost converter at the receiver side under perfect tuning condition. In this chapter, tri-state-boost converter and normal boost converter will be simulated in detuning situations.

As a result, the power converter for the tuning should adjust the input reactance to compensate the tuning tank, and the input resistance becomes the equivalent load resister in the above statement. So the voltage across the pick-up inductor and capacitor V_{ac} , which is also the input voltage of the rectifier with the power converter, should be in phase with the its input current and the receiver coil short circuit input current I_{sc}. In the end, when the power converter is working, the input power factor of the rectifier with the power converter should be unity power factor. This property can be used to design the circuit.

In this situation, a tri-state-converter is used here to regulate the real power flow and control the reactive power. Under CCM condition, tri-state-converter uses the free-wheeling of the inductor current to clear the input current when the normal boost converter switch (Sb) is switched off. This free-wheeling of the boost converter inductor current doesn't affect the input voltage phase while only input current changes according to the free-wheeling control. The input power factor can be controlled using this free-wheeling state.

According to reference [2], conventional boost converter in DCM can also work in three modes. It is not used in this power factor control situation because of the high order harmonics, difficulties to control, poor switch utilization and excessive switch stress.

Building a controlled pick-up capacitor tuning tank is a way to help improve the active tuning. The method to control free-wheeling switch signal won't work correct when the detection circuit doesn't produce the right results. With the active capacitor tank in the compensation network, the real capacitor functioning in the circuit changes will increase value when resonant frequency is higher than input frequency and decrease value when resonant frequency is lower. The input voltage of the receiver is V_{oc}, the voltage measured physically at the side of pick up coil is the voltage of capacitor and the parallel Z_{load}. This will be simulated in the next part.

3.2 Tri-state-boost converter

3.2.1 Introduction to tri-state-boost converter

The converter used after rectifier in this thesis is a tri-state-boost converter. The reason for choosing boost based topology is as follows.

For the basic buck or boost topology: Because the compensation circuit is determined to be parallel for the benefit of voltage boost function and current limitation property of the load branch over series compensation, the power converter input current of buck converter is discontinuous which needs an additional input filter. So boost topology converter is chosen here for the power flow control.

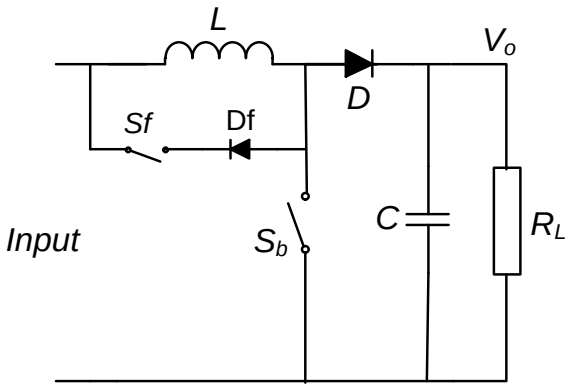

Figure 3-2 tri-state-boost converter topology

Traditionally, tri-state-boost converters are used to eliminate the famous right half plane zero of the conventional boost converter in CCM, but that way of control is not the focus of this thesis. Model is derived in this chapter according to[5].

Tri-state-boost converter in this thesis means when the boost converter is working in CCM, the switch control can divide the converter in two subintervals, switch on subinterval and switch off subinterval. During the boost converter switch on subinterval, current through the inductor doesn't go to the load side capacitor and load. During the switch off subinterval, current goes to the load side. When the switch is off , if the inductor current can have some free-wheeling time the current through the inductor will flows in its freewheeling loop staying at a constant value.

Tri-state-boost converter topology is shown in Figure 3-2 tri-state-boost converter topology, Components D_f and S_f are the free-wheeling diode and switch, S_b is the conventional boost switch. Normally tri-state-boost converter has three working conditions in CCM.

Free-wheeling mode shown in Figure 3-3 free-wheeling subinterval: when switch S_f is on and S_b is off, then the current flows in the loop of inductor L, switch Sf and diode D_f. Input current to the converter is zero.

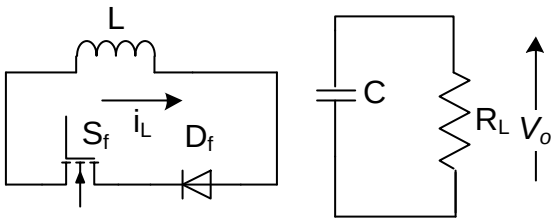

Figure 3-3 free-wheeling subinterval

Boosting mode (shown in Figure 3-4 boost subinterval): When switch Sf is off and switch Sb is on, it's storing energy in the inductor. Current goes through the inductor and into the ground.

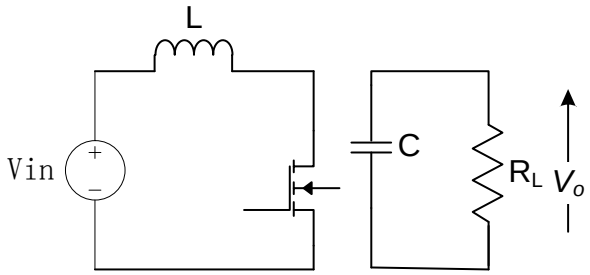

Figure 3-4 boost subinterval

Capacitor Charging Mode（shown in Figure 3-5 capacitor charging subinterval）: When switch Sf and Sb are both off, the current flows through the inductor and charge the output capacitor.

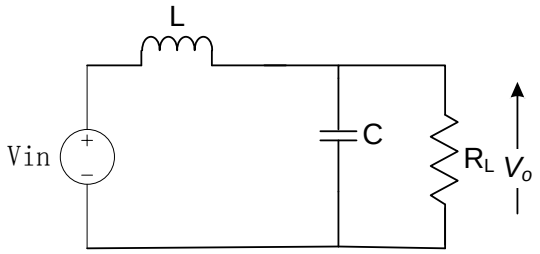

Figure 3-5 capacitor charging subinterval

In one period, the duty cycle of free-wheeling, boost and capacitor charging mode should meet $D_f + D_b + D_0 = 1$. Steady state analysis of the converter results in equations:

$$V_{out} = V_{in} \frac{1-D_f}{1-D_f-D_b} = \left(1 + \frac{D_b+D_f}{D_0}\right) V_{in} \quad [3.1]$$

$$I_L = \frac{I_{in}}{1-D_f} = \frac{I_o}{D_0} \quad [3.2]$$

where $I_L$is current of inductor L, I_o is the load current. At the end of this chapter, a steady state simulation analysis of the tri-state-boost with DC input will be presented. Inductor current should not designed very low because there is a boundary between working in two-state-boost and tri-state-boost [1].When the inductor current drops to the value of normal boost converter inductor value, then the free-wheeling state won't happen.

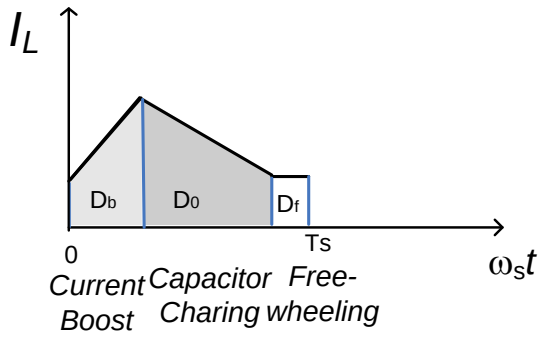

Figure 3-6 tri-state-boost inductor current waveform

Figure 3-6 tri-state-boost inductor current waveform shows the current of the inductor in one period when both switch frequencies are very high. D_f is the freewheeling duty cycle, D_b is the normal boost duty cycle, and D_0 the rest duty cycle. T_s is the switching period.

To achieve the power factor control, it is also reasonable to use a normal input current control boost power factor correction converter. But to control the input current using the PFC converter, the switching frequency of the switch should be much higher than the frequency of the input current waveform. For inductive power transfer system, the normal frequency of the input current is more than 20Khz. Then the corresponding switching frequency will be even higher, which will induce higher switching loss and EMI issue. The advantage of the tri-state-boost converter doesn't need the free-wheeling switch work in very high frequency. For example: if the pick-up current frequency is 100Khz, then the free-wheeling switch only needs to switch twice in each period of the 100Khz--at the beginning or the end of each half switching period.

3.2.2 Small signal model of tri-state boost converter (under CCM)

The small signal model of the tri-state-converter is derived in [5] using the signal flow graph modeling method. The method is very suitable for the multi-state converter [1], because each different state can be described in the signal flow graph and put together. When deriving the small signal model using the signal flow graph (SFG), Mason's gain formula makes it very easy to get the transfer function. This method will be used to derive the converter used with the parallel compensated receiver topology in next session.

Control to output transfer function of tri-state-boost converter according to[5]:

$$\frac{\widehat{v_o}(s)}{\widehat{d_b}(s)} = \frac{RV_g D_0}{[(SL+r)(1+SRC)+RD_0^2]} \quad [3.3]$$

$$\frac{\widehat{v_o}(s)}{\widehat{d_b}(s)} = \frac{RV_g D_0(1+SCR_c)}{[(SL+r)[1+SC(R+R_C)]+RD_0^2(1+SCR_c)]} \quad [3.4]$$

Equation [] is the same transfer function considering the output capacitor ESR R_c.

In the above equations, R is the load resister, C is the output capacitor, D_0 is the capacitor charging subinterval duty cycle steady state value, V_g is the input voltage, V_o the output voltage and r the resistance of the inductor L.

From the equation 3.3, it is very clear tri-state-boost converter doesn't have the RHP as the conventional boost converter.

3.3 Parallel compensated receiver with tri-state-boost converter

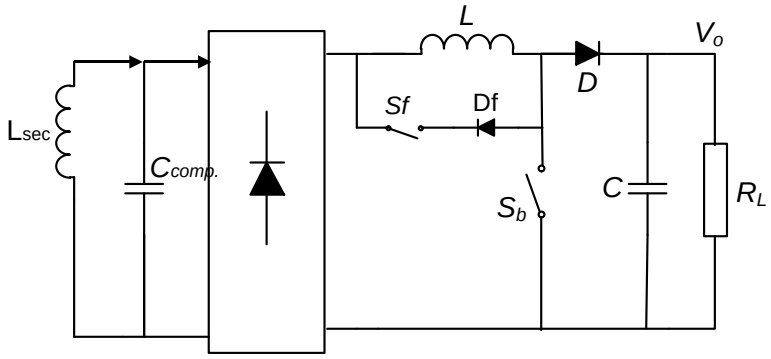

Figure 3-7 parallel compensated tri-state-boost receiver topology

Unlike the ideal DC transformer model in chapter 2 discussed in boost converter, the bridge rectifier input current is discontinuous in the tri-state-boost condition. The turn ratio value n

for the new DC transformer model should consider change because of the equavalent current input current of the rectifier Iac under the free-wheeling duty cyle D_f control influence.[1]

Reference article [2] gets the control-output transfer function for the receiver using the SFG method like article [5] and recommends a controller for that. The result is:

$$G_{vd}(s) = \frac{\widehat{v_0}}{\widehat{d_b}} = \frac{-R_L(S^2 I_L L C_{comp,} + \alpha S + \beta)}{(\gamma S^3 + \delta S^2 + \varepsilon S + (D_0 + D_b)^2)} \quad [3.5]$$

$$\alpha = -C_{comp.} V_0 D_0 \quad [3.6]$$

$$\beta = I_L (D_0 + D_b)^2 \quad [3.7]$$

$$\gamma = LC_{comp.} C R_L \quad [3.8]$$

$$\delta = LC_{comp.} \quad [3.9]$$

$$\varepsilon = C R_L (D_0 + D_b)^2 + D_0^2 R_L C_{comp.} \quad [3.10]$$

Where $I_L = \frac{I_{dc}}{(D_0 + D_b)}$, $V_o = V_{ac} \frac{(D_0 + D_b)}{D_0}$ the steady state inductor current and output voltage without taking DC resistance of the inductor and output capacitor ESR into account. There is a negative sign similar to the boost receiver case. The transfer function shown above has double poles and double right half plane zeros. Traditional controller design is very complicated. Voltage mode output voltage hysteresis control is always stable for the CCM boost converter, so it is used here for simplicity and robustness.

Effect of detune and active tuning：Considering the free-wheeling duty cyle's influence to the input voltage and current, take the first harmonic of them to analysis, the injected impedence of the tri-state-boost converter can be calculated as expalined in the following paragraph.

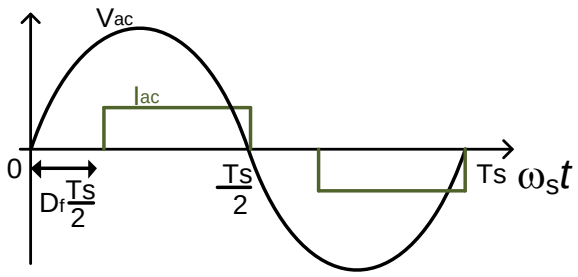

Figure 3-8 V_{ac} and I_{ac} waveform under free-wheeling switch control waveform

If the position Df is at the beginning of each half switching period like Figure 3-8 V_{ac} and I_{ac} waveform under free-wheeling switch control waveformshows， then relation between V_{ac} and V_o, and relation between I_o and I_{ac} are:

$$V_{ac,rms} = \frac{\pi D_0}{\sqrt{2}(1+cosD_f\pi)(1-D_f)} V_o \quad [3.11]$$

$$I_{ac} = \frac{2\sqrt{2}\, I_o \cos(\frac{D_f\pi}{2})}{\pi D_0} e^{-\frac{D_f\pi}{2}} \quad [3.12]$$

Tri-state-boost coverter with the free-wheeling duty cycle Df can cause a $\frac{D_f}{2\pi}$ phase delay to the input current when placed at the beginning of each period, and lead $\frac{D_f}{2\pi}$ phase when placed at the end of each period.

According to reference[1], the new converter, conventional boost converter and LC filter injected impedence at the resonant tank are listed in Table 3.3-1 injected impedance of tri-state-boost converter, boost converter and filter: In a word, traditinoal boost converters at the receiver using D_0 and D_b dynamically switch on load resister R_L branch to mimic a smaller load resister for tuning tank. With a free-wheeling it can dynamically put an injected C_{ac} there, affecting the input voltage—similar to load resistior open circuit.

Rectifier voltage magnitue increases V_{ac} with D_f,which is good for tuning tank voltage detection, but it will not influence the equavalent voltage input V_{in} to the converter and output voltage V_o.

Detune effect : Reference [3] defines tuning factor and detuning factor to illustrate the change of output power and voltage when detuning happens.

For LC filter situation, ouput voltage and power can only get the maximum under normal conditions.

Table 3.3-1 injected impedance of tri-state-boost converter, boost converter and filter

Parameter	Tri-state-boost	Normal boost	Filter
R_{ac}	$\frac{\pi^2}{8}\frac{D_0^2 R_L}{(1-D_f)cos^4(\frac{D_f\pi}{2})}$	$\frac{\pi^2}{8}(1-D_b)^2 R_L$	$\frac{\pi^2}{8}R_L$
C_{ac}	$-\frac{\pi^2}{8}\frac{(1-D_f)cos^3(\frac{D_f\pi}{2})\sin}{D_0^2 R_L \omega_0}$	0	0

For the normal boost situation, the boost converter has a boost switch duty cyle to control. When detune happens, the capacitor charge subinterval duty cycle of the boost converter D_0 changes from the tuning case value $D_{0,0}$. To achieve the controlled ouput DC voltage and power, the converter will decrease the boost duty cycle to achieve the maximum output power until it gets to 0 as a filter when absolution of detuning factor defined as

$$\Lambda d = Q_0(\frac{C_{comp}}{C_{comp,o}} - 1) \quad [3.13]$$

is less than 0.5, where Q_0 is the condition resonant tank quatlity factor, $C_{comp.}$ the compensation capacitoance and $C_{comp,0}$ the perfect tuning compensation capacitance. But when absolut value of detuning factor is larger than 0.5, boost controller will not be able to get the expected voltage and power output. This can also be shown in simulation.

When detuning situation is really serious as the detuning factor is larger than 0.5, tri-state-boost is proved to be able to make the converter get the expected output power and voltage. [6] The reflected impedence remains constant resistive R_{ac}, and voltage measured across compensation capacitor V_{ac} remains the same when detuning happens. Tri-state-boost converter's property to actively tune the circuit can get the expected power better than the conventional boost converter. But for hysteresis control if the corresponding filter case output voltage smaller than the hysteresis band up limit, even when the detuning factor is smaller than 0.5, the boost converter receiver still won't trigger the control.

3.4 Controller design

Conditions of: minimum reactive power, resonant frequency of the LC tank ω_0 equals the input frequency, and unity rectifier input power factor are equivalent statement of tuning condition. Reference [6] suggests a novel control method to actively tune the circuit.

V_{oc} is the open circuit voltage of pick-up coil which is in phase with the transmitter voltage. V_{ac} is the voltage across the compensation capacitor when the receiver is working. V_{oc} leads the resonant tank voltage V_{ac} by 90°when the receiver is perfectly tuned. When the wireless power transfer system is not perfect tuned, ω_0 is not equal to ω. At this time if the resonant tank is capacitive under the input current frequency, V_{oc} leads V_{ac} more than 90°. If the resonant tank is inductive under the input current frequency, then the leading angle should be less than 90°. And V_{oc} will always leads V_{ac}. This character can be used to detect if the receiver is tuned or not.

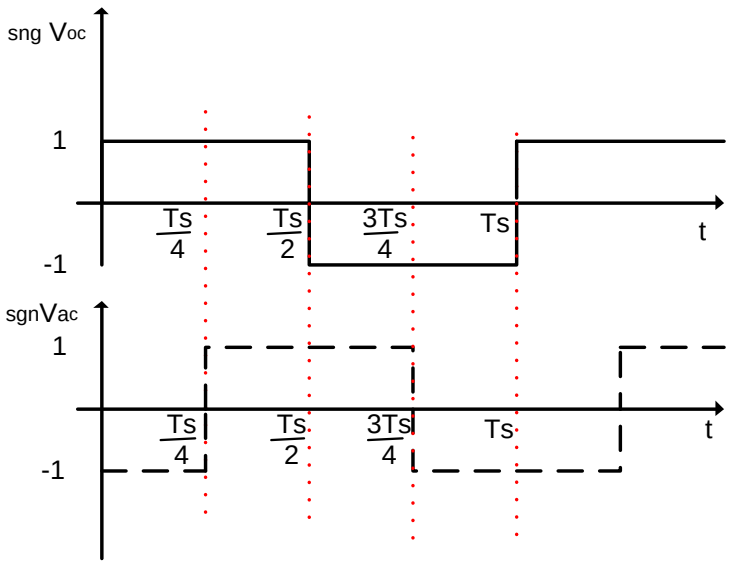

Figure 3-9 the sign of V_{oc} and V_{ac} in time scale under tuning condition

From Figure 3-9 the sign of V_{oc} and V_{ac} in time scale under tuning condition, the up one is the polarity of the voltage V_{oc}, and the bottom one is the one of V_{ac}. Value 1 means the polarity is positive and -1 the negtive. Under the perfect tuning condition, V_{oc} leads V_{ac} by 90, then the product of their signs integreted in one period should be 0.When detune happens, if the resonant tank under the given current input frequency is capacitive, the phase angel between V_{oc} and V_{ac} which is smaller than 90° will leads to the integretion result positive. D_f the free-wheeling subinterval positioned in the beginning of each half period of rectifier input AC voltage waveform will induce a phase lag to the input current—which means the tri-state-boost brings inductive part in the circuit. If the injected negtive reflected capacitance

absolute value is big enough, detune of the resonant tank will be compensated by the tri-state-boost. V_{ac} and V_{oc} relation:$V_{ac} = V_{oc}\frac{\frac{R_{ac}}{R_{ac}(1-\omega_s^2 C_{comp} L_{sec})+j\omega_s L_{sec}}}{}$ [2].

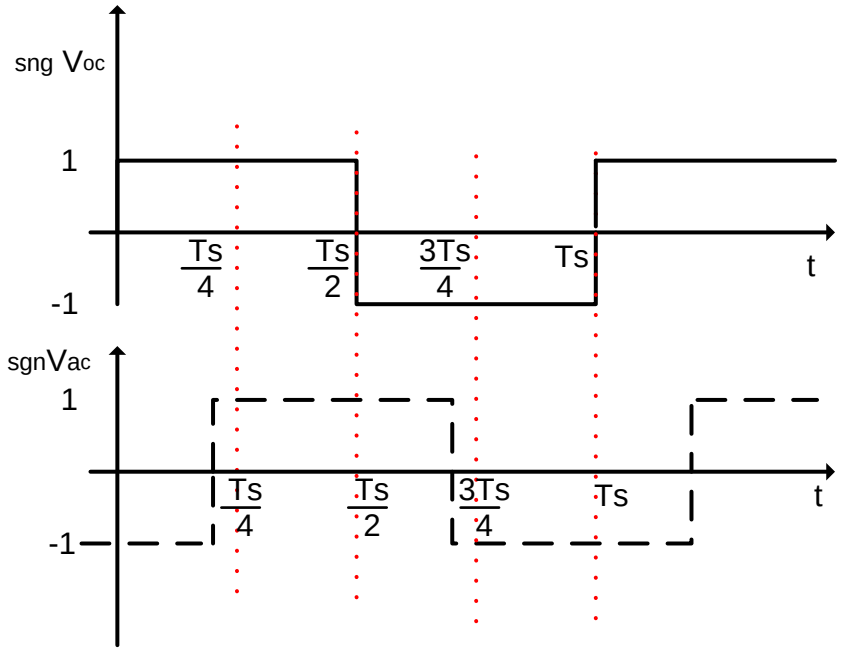

Figure 3-10 the sign of V_{oc} and V_{ac} in time scale when resonant tank is capacitive

And similarly if the resonant tank is inductive,tri-state-boost needs to inject a reflected capacitor to tune the circuit. Then the integration result of the product of V_{oc} and V_{ac} in one period will be negtive. In this case D_f needs to be placed at the end of each period.

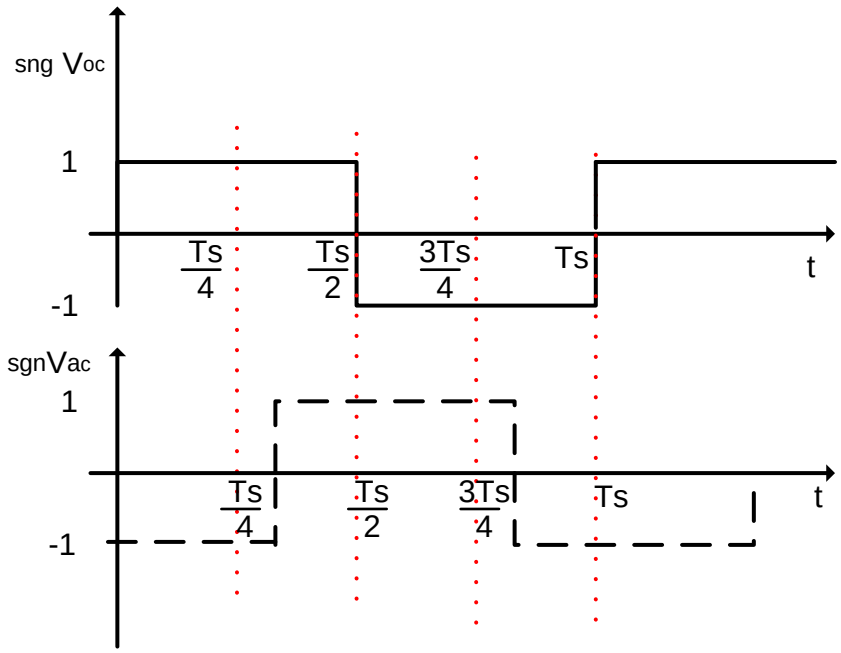

Figure 3-11 the sign of V_{oc} and V_{ac} in time scale when resonant tank is inductive

Voltage control uses hysteresis control and tuning control is to calculate the free-wheeling duty cycle for switch S_f. Hysteresis control duty cyle and frequency will change according to the position change of the pick-up coil, because of the change of the input voltage of the receiver. Free-wheeling control pwm frequency need to be synchrounized to the frequency of

V_{ac}, at twice the frequency of V_{ac}. But the voltage control frequency is not necessarily synchrounized to the V_{ac} frequency. In reference article[1], the controller for real power is a PID type with some hundreds hertz cut off frequency generating D_b pwm signal in 20Khz. The free-wheeling period is intentionally placed in each period which will never overlap with the D_b subinterval , shown in Figure 3-9 the sign of V_{oc} and V_{ac} in time scale under tuning condition.Although D_f is at very high frequency, its variation is at a very low frequency. So the two control loop coupling problems is neglected.[1]

In the hysteresis control situation: for the real-time control to generate D_f, controller firstly needs to capture the start of each V_{ac} period, and calculte the value of D_f according to the strategy discussed above. Secondly to avoid D_f and D_b overlap in one period, if overlap, then the free-wheeling duty cycle will automatically delayed. Practically, D_b under hysteresis control frequency changes (at about 10 Khz) according to the practical value of V_{ac}, (when hysteresis band and converter is not changed) sometimes taking much of the V_{ac} period and not synchronized to its frequency. For system 100Khz electrical magnetical frequency, free-wheeling control pulse apears at about 200Khz. Then during these periods, when freewheeling switch S_f and boost control switch S_b are on at the same time, current will not free-wheel in the inductor. When S_b switches off, controller will control S_f to create a biger C_{ac} to maintain the ballance.

Steady state analysis of the tri-state-boost shows that when the very short time D_f interrupts the D_b time, turning off-S_b just cause some delay to the D_b and D_o without any influence of the output voltage and power. Equation[43page] shows that output voltage is only affected by

the input voltage of the converter and D_o, D_b times. But simulation result reveals that the output voltage is out of control in that case, so the voltage should be controlled primarily and the free-wheeling control will be automaically extended when D_f and D_b overalap.

There are difficulties to detect the polarity of voltage V_{ac} practically, since during some time V_{ac} magnitude is zero as not the zero crossing points. This happens especially when switching frequency is low. If output capacitance is big, input voltage V_{oc} is low or the output voltage hysteresis band is too wide, switching frequency will not be very high. In the end, V_{ac} is always zero in the long S_b switch-on subinterval, and polarity detection result of the waveform is not suitable for the reactive control. In that case the integration of the two corresponding waveforms in one V_{ac} period is still zero cause V_{ac} is always zero, and the free-wheeling switch is not working. So overall, the reactive power control is working even in low switching frequency case.

When switch S_f is on, V_{ac} waveform magnitude will increase to be good enough for the following polarity detection work.

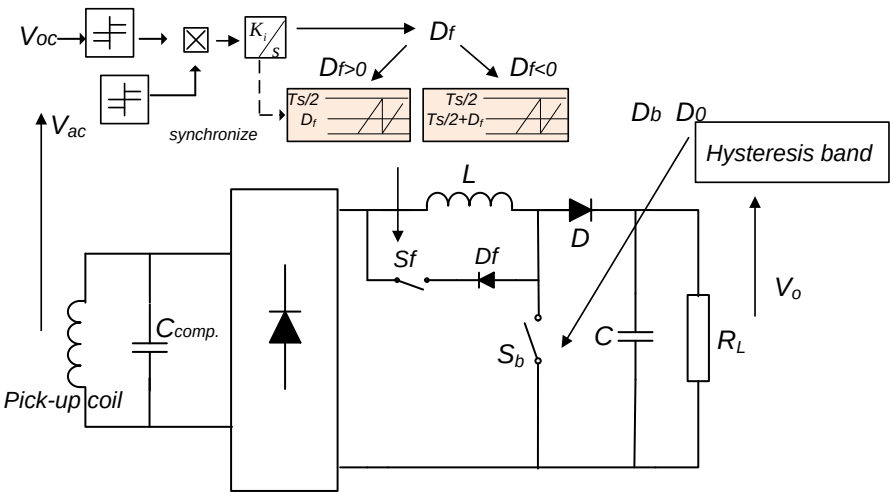

Figure 3-12 tri-state-boost converter receiver control

3.5 Simulation Summary

3.5.1 Boost converter at receiver side under detuning condition

$\Lambda d = Q_0(\frac{C_{comp}}{C_{comp,o}} - 1)$ is less than 0.5, boost converter can always achieve the corresponding LC filter nominal power output[]. In this step, change the compensation capacitor $C_{comp.}$ to

$C'_{comp.1} = C_{comp.0}(1 + \frac{1}{3R_L}\sqrt{\frac{L_{sec}}{C_{comp.0}}})$

From the Figure 3-13 V_{ac}, control signal, I_L and V_{out} waveforms of boost converter receiver with a $\frac{1}{3}$ detuning factor above, boost converter with $\Lambda d = \frac{1}{3}$ condition different from tuning condition will produce more reactive power in the tuning tank, but it can still have the

expected output voltage and power. It doesn't make sense because the controlled output power is essentially smaller than the corresponding LC filter nominal output power.

1: slightly detune condition

Table 10 simulation paramters of boost converter receiver with a $\frac{1}{3}$ detuning factor

Parameter	Symbol	Value	Unit
Pick-up Coil Open Circuit Voltage	V_{oc}	6 (AC Peak)	V
Secondary Coil self-inductance	L_{sec}	23.8	μH
Compensation Capacitance	$C^{1}_{comp.1}$	116.8	nF
Boost Converter Inductance	L	120	μH
Boost Converter Capacitor	C	22	μF
Boost Load Resistance	R_L	51	Ω

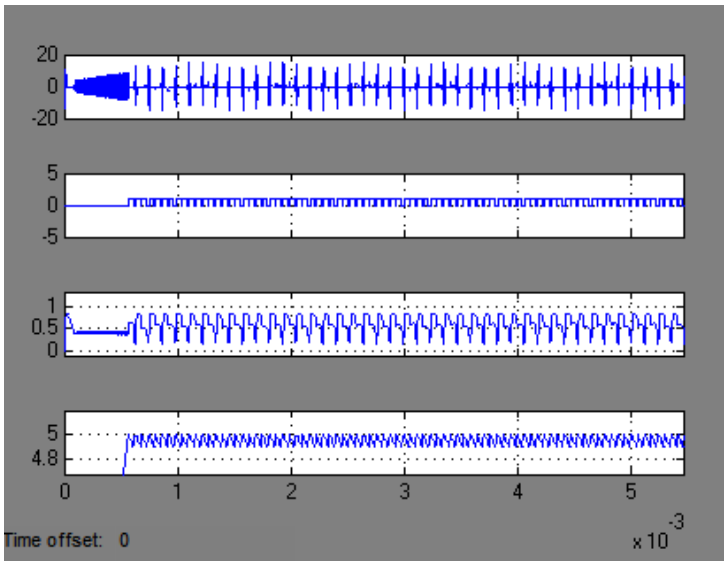

Figure 3-13 V_{ac}, control signal, I_L and V_{out} waveforms of boost converter receiver with a $\frac{1}{3}$ detuning factor

Step 2: heavily detune condition

When the compensation capactiance is 160nF, then the value of Λd is 1.72. This is a heavily detuned system receiver. The corresponding LC filter power output in this compensation situation is smaller than the hysteresis control band up limit. This case, the converter will never have the output power.

The Figure 3-14 V_{ac}, control signal, I_L and V_{out} waveforms of boost converter receiver with a 1.72 detuning factor above shows that boost converter at receiver side with detuning factor $\Lambda d = 1.72$ can't produce the expected output voltage and power. The boost switch duty cycle D_b is always 0. However, in the next part with tri-state-boost converter, the output voltage can get to the expected value.

Table 3.5-1 simulation paramters of boost converter receiver with a 1.72 detuning factor

Parameter	Symbol	Value	Unit
Pick-up Coil Open Circuit Voltage	V_{oc}	6 (AC Peak)	V
Secondary Coil self-inductance	L_{sec}	23.8	µH
Compensation Capacitance	$C^2_{comp.1}$	160	nF
Boost Converter Inductance	L	120	µH
Boost Converter Capacitor	C	22	µF
Boost Load Resistance	R_L	51	Ω

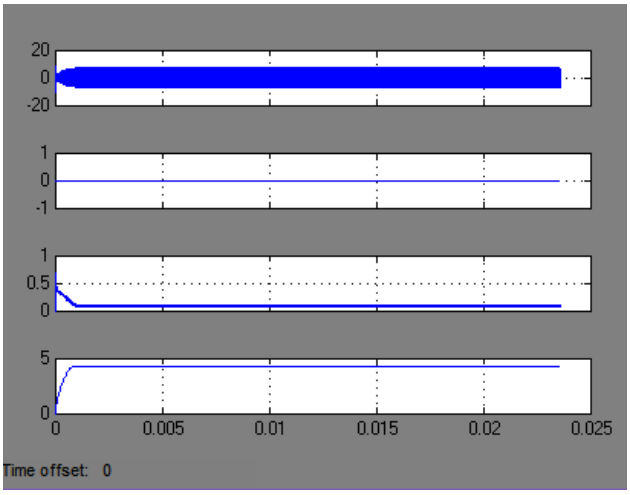

Figure 3-14 V_{ac}, control signal, I_L and V_{out} waveforms of boost converter receiver with a 1.72 detuning factor

3.5.2 Tri-State-Boost converter at receiver side

Simulation block diagram of the receiver in Simulink is shown in Figure 3-15 Simulation block diagram of the tri-state-boost receiver.

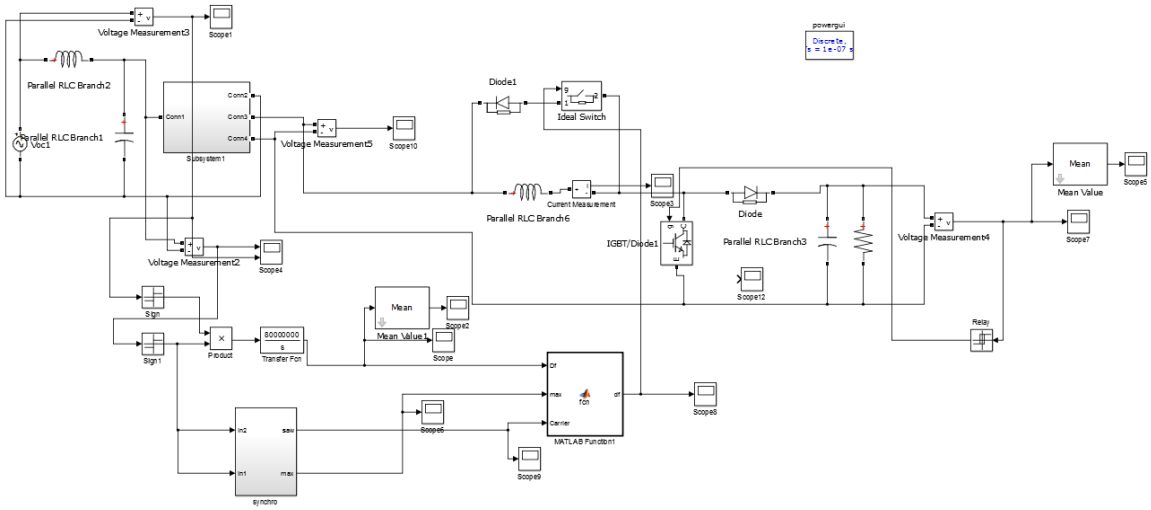

Figure 3-15 Simulation block diagram of the tri-state-boost receiver

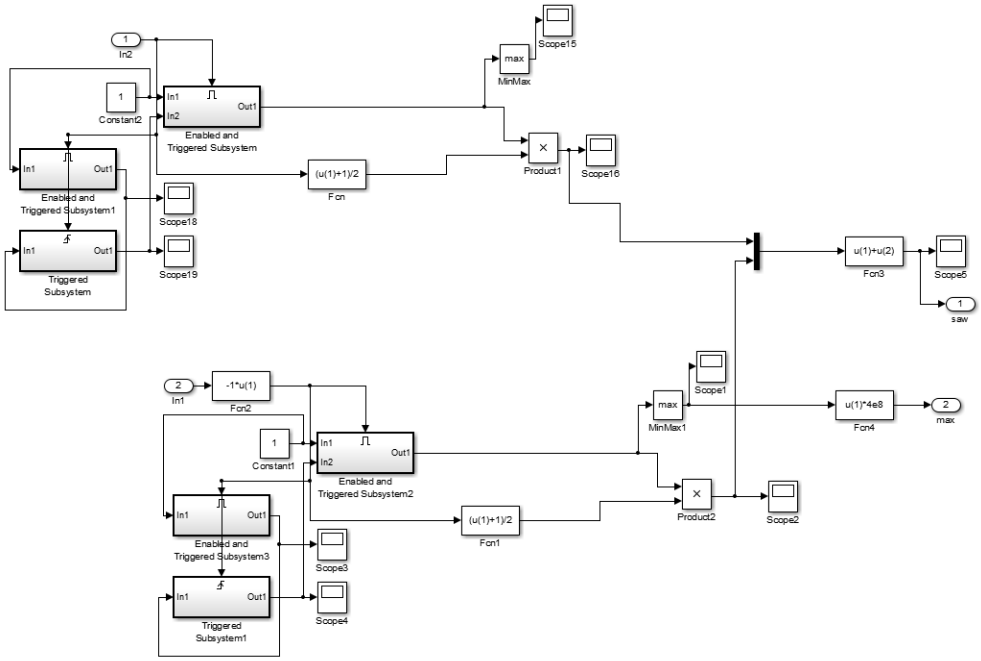

Figure 3-16 Synchronization block for V_{ac} and D_f waveform

The simulation plot of tri-state-boost converter is quite similar to the conventional boost one. But it is very important that the control signal of D_f should be synchronized to the frequency of the rectifier output voltage at about 200Khz. When generating the control signal, reference waveform is from the integration result, the carrier should be synchronized to the detection waveform of V_{ac}. It can be achieved like the way shown in Figure 3-16 Synchronization block for V_{ac} and D_f waveform. The carrier waveform is changing constantly meaning the V_{ac} waveform is always changing. This can be explained by the control signal of boost switch D_b in low frequency and the influence of the D_f control. Like the Figure 3-17 Carrier waveform for generating free-wheeling control signal shows, carrier waveform and V_{ac}

waveform are changing because sometimes being short circuited and sometimes being influenced by the C_{ac}.

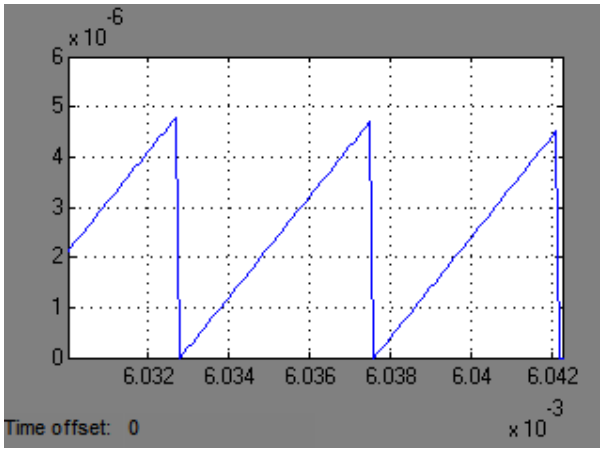

Figure 3-17 Carrier waveform for generating free-wheeling control signal

Figure 3-18 The resulting output voltage of tri-state-converter receiver with a 1.72 detuning factorshows the resulting output voltage. Tri-state-boost in this detune condition can still get the expected output voltage. The integration result for generating the D_f is shown in Figure 3-19 free-wheeling control signal, converter inductor current and integration result waveform of tri-state-boost converter, while the integration result in tri-state-boost condition is shown in Figure 3-20 the integration result waveform of tri-state-boost converter receiver with an active capacitor tank. It's obviously that tri-state-boost can help actively tune the circuit.

Simulation:

From the Figure 3-19 free-wheeling control signal, converter inductor current and integration result waveform of tri-state-boost converter showing the integrating result for D_f， inductor current and the control signal D_f waveform, the system is working in CCM. Sometimes D_f is always on, and that is because D_b affects the D_f by conducting all the inductor current to the ground in steady of free-wheeling, thus leaving a longer S_f switch on time.

Table 3.5-2 Simulation parameters of tri-state-boost converter with a 1.72 detuning factor

Parameter	Symbol	Value	Unit
Pick-up Coil Open Circuit Voltage	V_{oc}	6 (AC Peak)	V
Secondary Coil self-inductance	L_{sec}	23.8	μH
Compensation Capacitance	$C^2_{comp.1}$	160	nF
Boost Converter Inductance	L	120	μH
Boost Converter Capacitor	C	22	μF
Boost Load Resistance	R_L	51	Ω

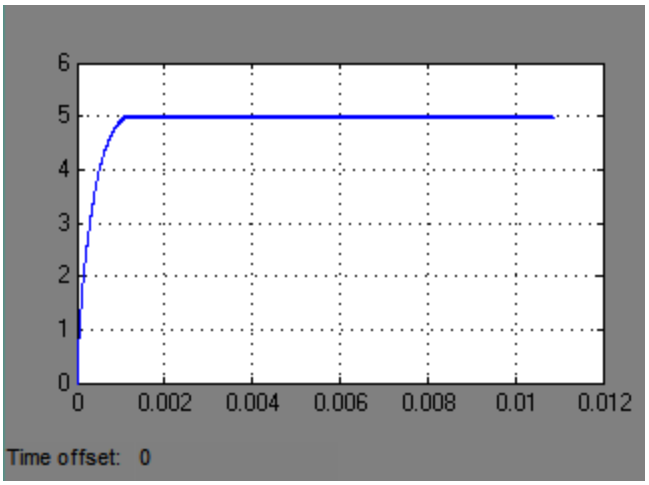

Figure 3-18 The resulting output voltage of tri-state-converter receiver with a 1.72 detuning factor

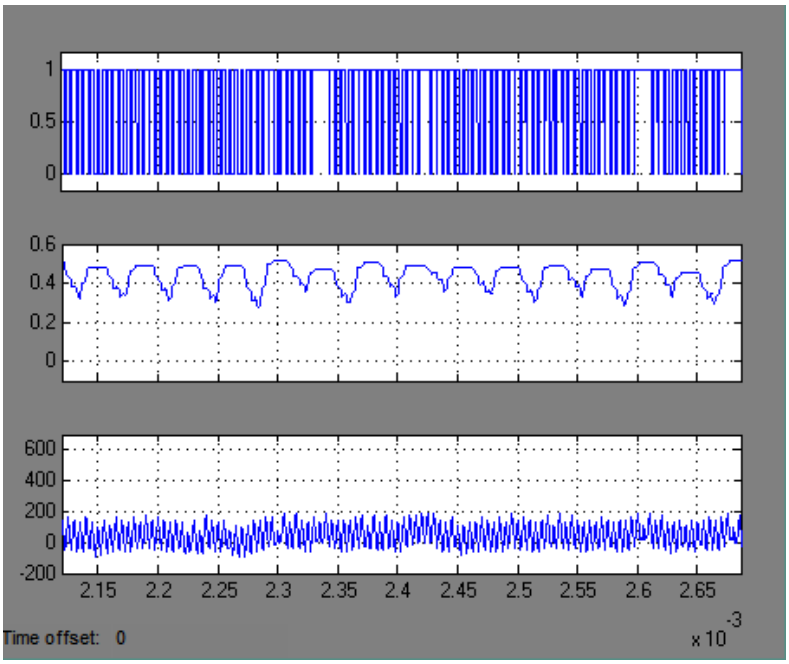

Figure 3-19 free-wheeling control signal, converter inductor current and integration result waveform of tri-state-boost converter

The tri-state-boost converter ideally should actively tune the circuit even in very detuned condition when detuning factor Λ_d is very large. But there is a case when the signal D_f control fails when the D_f sometimes is positive over 50% and sometimes smaller than -50%. That's means because of the control is not designed for every condition so sometimes the switch S_f will be always on in heavily detuned condition. When switch S_f is always on, tri-state-boost control fails. The receiver then will be the same as the filter case.

So, an active picking-up tank is used here to make sure the active tuning works fine. When integration result's absolution value is over some value, the picking-up tank shown in Figure 4-11 pick-up circuit with active capacitors tank can actively add or reduce a shunt capacitor. In simulation where the compensation capacitor is 80 nF, tri-state-boost converter alone fails in simulation. However, If a 20nF capacitor is connected parallel to the compensation capacitor when integration result is bigger than 300, then the tri-state-boost can works normally with the integration result shown in Figure 3-20 the integration result waveform of tri-state-boost converter receiver with an active capacitor tank. (Actually, the capacitor is always connected to the tank like the compensation capacitor $C_{\text{comp.}} = 120nF$ case, with a positive integration result meaning capacitive resonant tank)

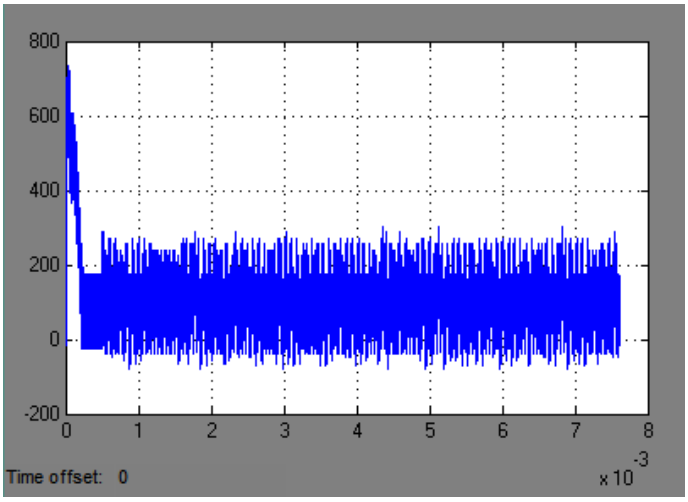

Figure 3-20 the integration result waveform of tri-state-boost converter receiver with an active capacitor tank

4 Chapter 4 Experimental Setup

4.1 Transmitter Components

1 Primary Coil and Pick-up Coil

Table 4.1-1 Parameters of primary coil and secondary coil

Parameter	Symbol	Value	Unit
Primary coil self-inductance	L_t	24.03	μH
Primary coil ESR	R_t	178	mΩ
Primary coil quality factor	Q_t	33.86	1
Pick-up coil self-inductance	L_{sec}	23.8	μH
Mutual inductance (normal)	M	7.96	μH
V_{oc} sense coil self-inductance	L_{voc}	9.7	μH

Primary Coil is shown in Figure 4-1 primary coil size, number of layer and turnswith the parameters:

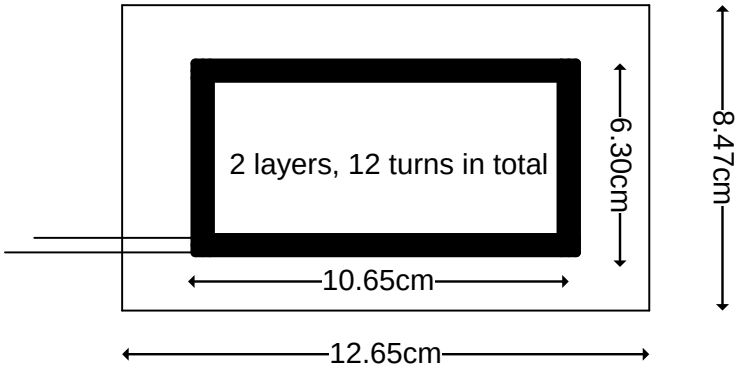

Figure 4-1 primary coil size, number of layer and turns

2 Transmitter for Inductive Power Transfer System

As the results simulation in the simulation showed the steady state value of the current and voltages in Table 4.1-2 Steady state values of the current and voltages of transmitter components.

For the circuit components:

Mosfets: the four switches undertake 4V and flow 2A at most in the result of Simulink. So the mosfets chosen for the hardware are Texas Instrument CSD17308Q3. It can undertake maximum 30V drain to source voltage V_{ds} and maximum 13A drain current. Turn-off delay time is 9.9ns, which won't have big influence to the 100Khz switching frequency performance.

Table 4.1-2 Steady state values of the current and voltages of transmitter components

Parameter	Symbol	Value(AC Peak)	Unit
Transmitter Coil Current	I_{t}	0.816	A
Series Capacitor Voltage	$\mathrm{V_{cseries}}$	12.23	V
Series Inductor Current	$\mathrm{I_{Lseries}}$	2.026	A
Parallel Capacitor Voltage	$\mathrm{V_{cpara}}$	12.15	V

Gate driver IC is the Texas Instrument TPS28225 for the full bridge four N-channel Mosfets with 14ns adaptive deadtime. Gate voltage is 4.5V to 8.8V which matches the four mosfets. Input PWM signals can accepts 2.0V to 13.2V as logic high, this can directly connect the DSP output or other 5V IC CMOS output. Charge and discharge the gate as high-current 2A source and 4-A sink. With boot-strap function, two TPS28225 ICs can drive the two high side switches and two low side switches of the full bridge. Simulation in Pspice is presented as follows.

Capacitors are chosen in ceramic surface mount package with 50V rated value and $\pm 10\%$ tolerance. SMD Ceramic capacitors have smaller ESR than other types and the transmitter circuit needs all the capacitors used in AC conditions. X7R or X5R capacitors are more stable with frequency and temperature changes than other types and the tolerance is smaller.

In addition, X5R and X7R ceramic capacitors have extremely low ESR with typical values less than 5mΩ according to the datasheets.

Inductor is chosen in surface mount with 6A rated current and 17Mhz self-resonant frequency.

3 Simulation In PSpice:

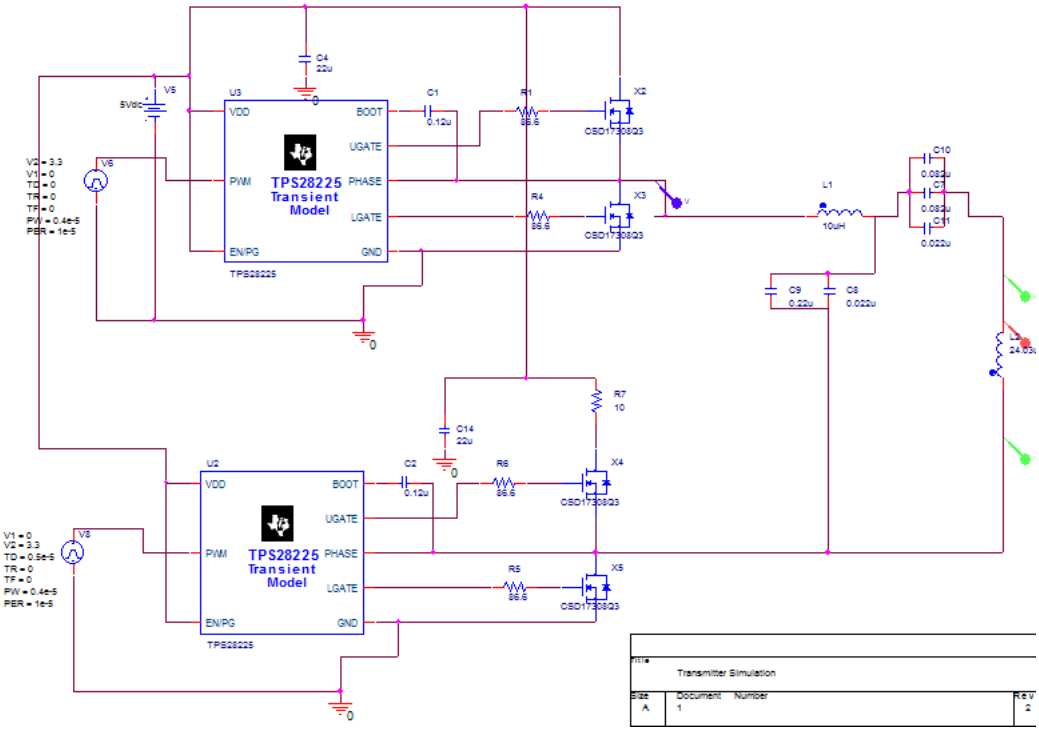

Figure 4-2 PSpice simulation of the transmitter

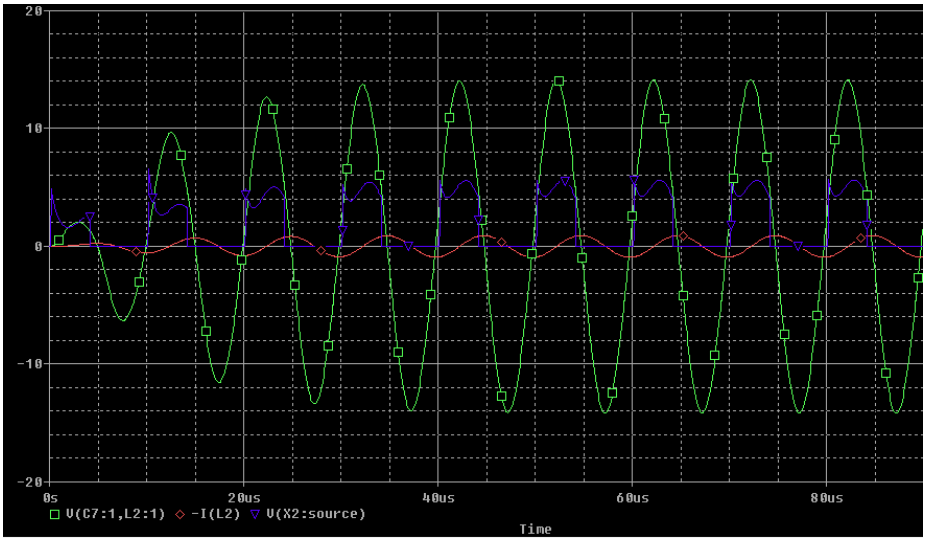

Figure 4-3 PSpice simulation result of the transmitter circuit (green line—coil voltage, red line –coil current, blue line low side mosfet V_{ds})

The components in Pspice simulation are tested to be ok.

4.2 Receiver Components

As the results simulation in the simulation showed the steady state value and approximate maximum value in the same way as the receiver circuit. The maximum value of capacitor voltage is the voltage of $C_{comp.}$ with 18V and maximum current is 1.5A. So the capacitors are chosen X7R and X5R ceramic surface mount capacitors with 50V rated voltage. Receiver coil is Wurth Electronics 23.8µH with rated current 6A one layer one coil. The saturation current is 10A which is not a problem for this low power scale project. DCR is smaller than 100mΩ.

Figure 4-4 Transmitter coil

Bridge rectifier is composed of four Schottky fast recovery diodes STPS2L60RL with 60V rated voltage, 2A rated current and 600mV maximum voltage drop.

The boost converter switch undertakes maximum voltage of 18V and maximum current 0.6A with lower switching frequency than the transmitter, so it also uses Texas Instrument Mosfet CSD17308Q3 here with the gate driver TPS28225.

Boost converter inductor is a120μH surface mount inductor SRR1280 with rated current 1.95A.

Diode is FYD0504SA schottky diode with maximum reverse voltage 40V and 5A rated current. The maximum forward voltage drop in this low current situation is less than 550mV.

Resisters: R_1 is a 18Ω, 2W resister and R_2 a 33Ω, 2W resister. Connection of the resisters is shown in Figure 4-5 voltage divider feed-back for TMS320F28335 ADC module.

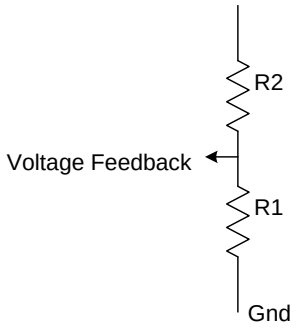

Figure 4-5 voltage divider feed-back for TMS320F28335 ADC module

4.3 Receiver design

4.3.1 Schematics

1 The pick-up compensation and rectifier:

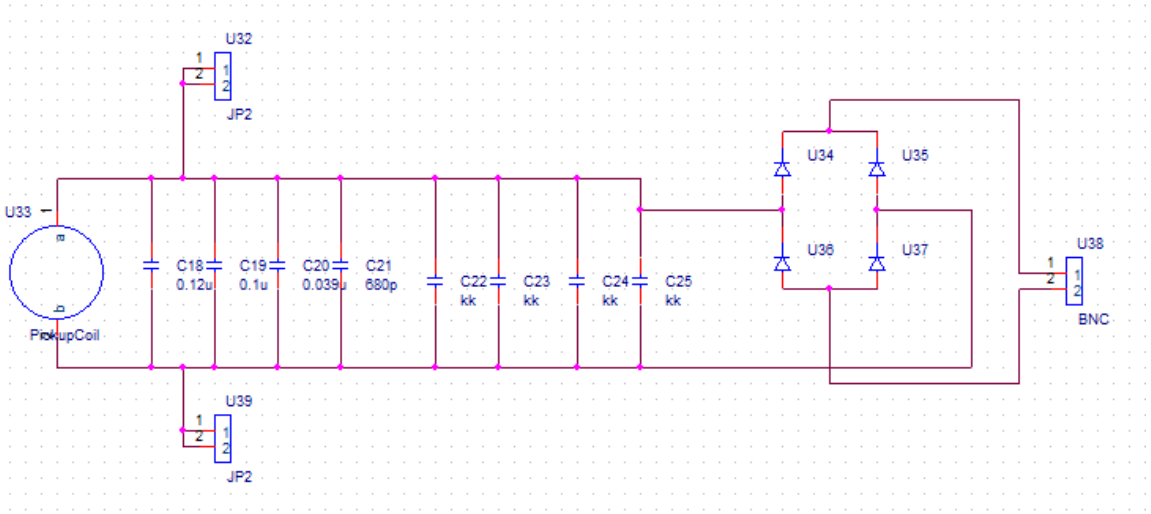

Figure 4-6 pick-up compensation and rectifier circuit

2 The tri-state-boost:

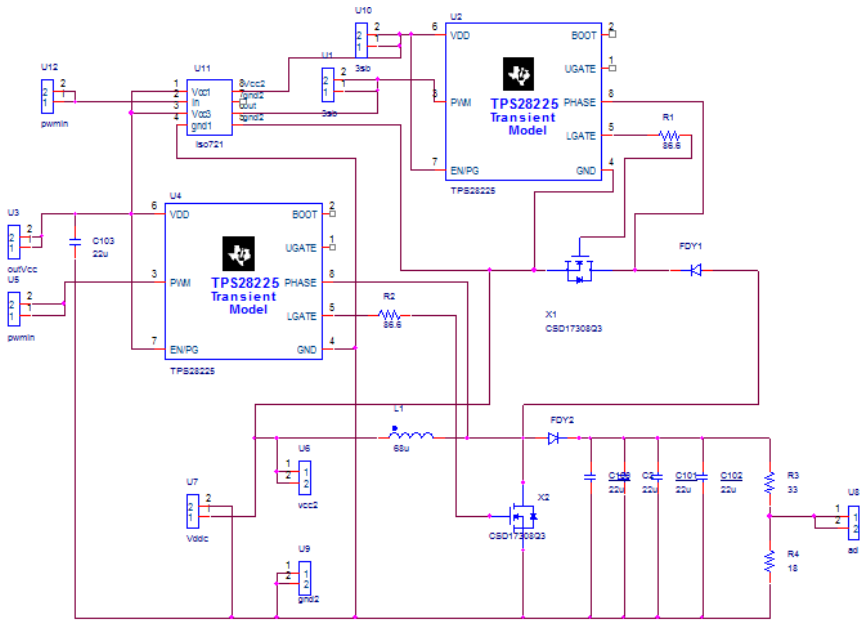

Figure 4-7 tri-state boost circuit

3 The voltage cross zero detection:

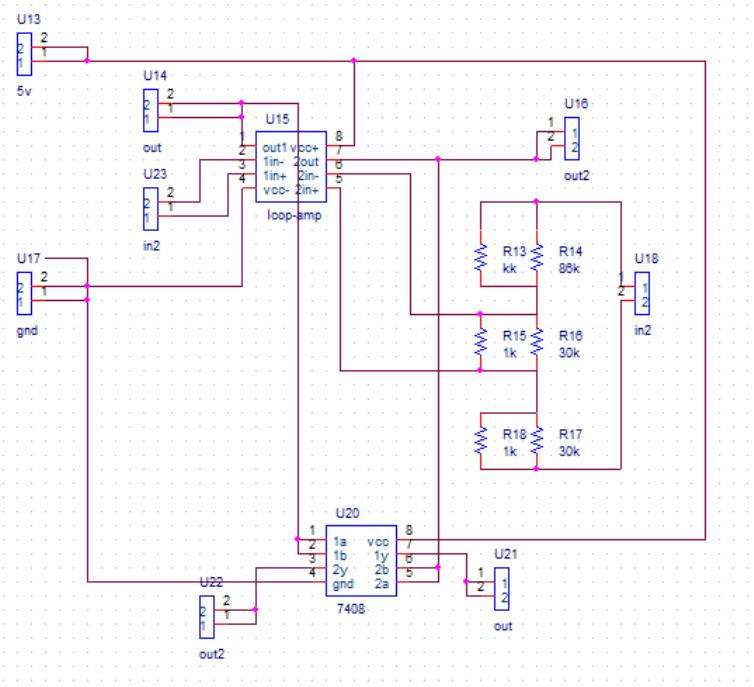

Figure 4-8 voltage zero-crossing detection circuit

Op-amp should have high gain-bandwidth. A positive And gate 7408 is used here at the output of op-amp. According to Application note [10], Op-amp with And gate can be used as a comparator. In the end, to limit the output circuit and smooth the output waveform, 800Ω resister will be connected in series between the detection output pins and DSP input pins.

In addition, the circuit to providing pwm control signal from signal generator to transmitter full bridge can be either one of the following circuits, so the transmitter can be directly controlled by signal generater:

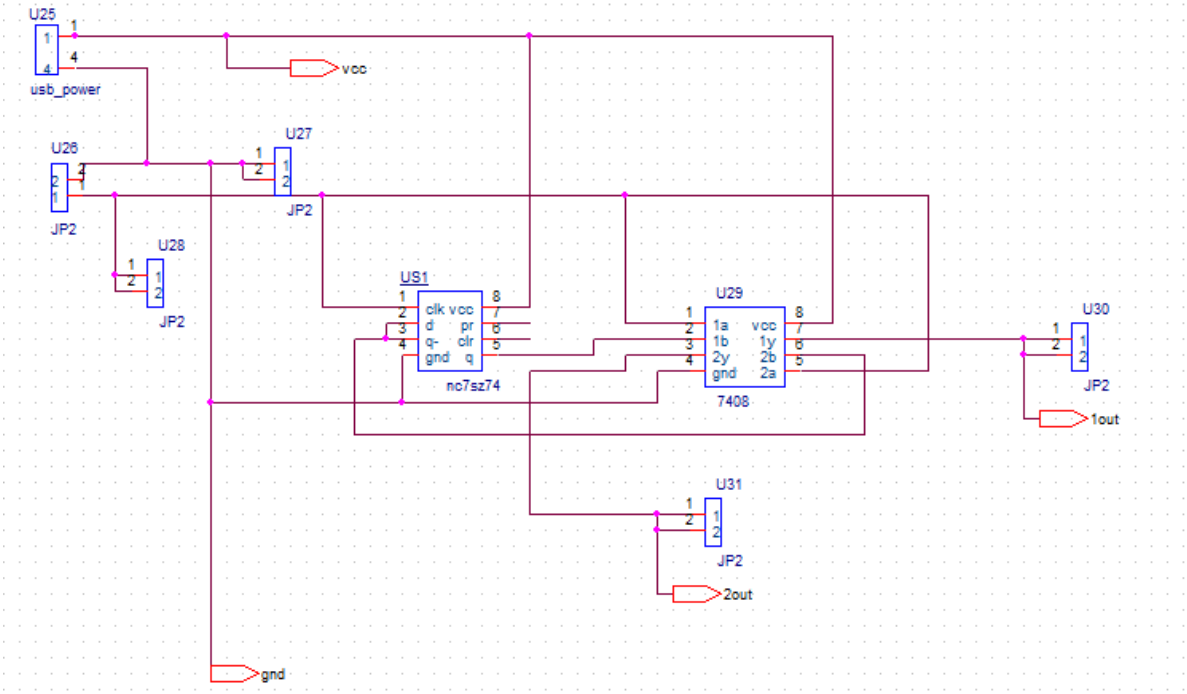

Figure 4-9 control signal circuit 1 for transmitter full-bridge

This circuit requires the signal generator produce twice of the coil current frequency， or another circuit with Delay IC LTC6994-2 can be used:

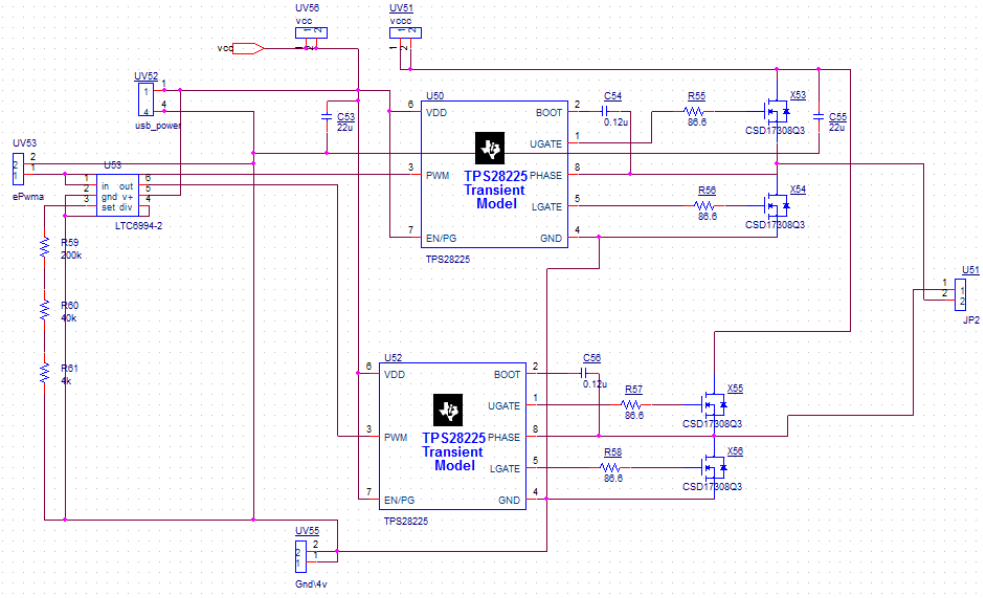

Figure 4-10 Control signal circuit 2 for transmitter full-bridge using delay IC

4 Active capacitor tank schematic is shown below in Figure 4-11 pick-up circuit with active capacitors tank.

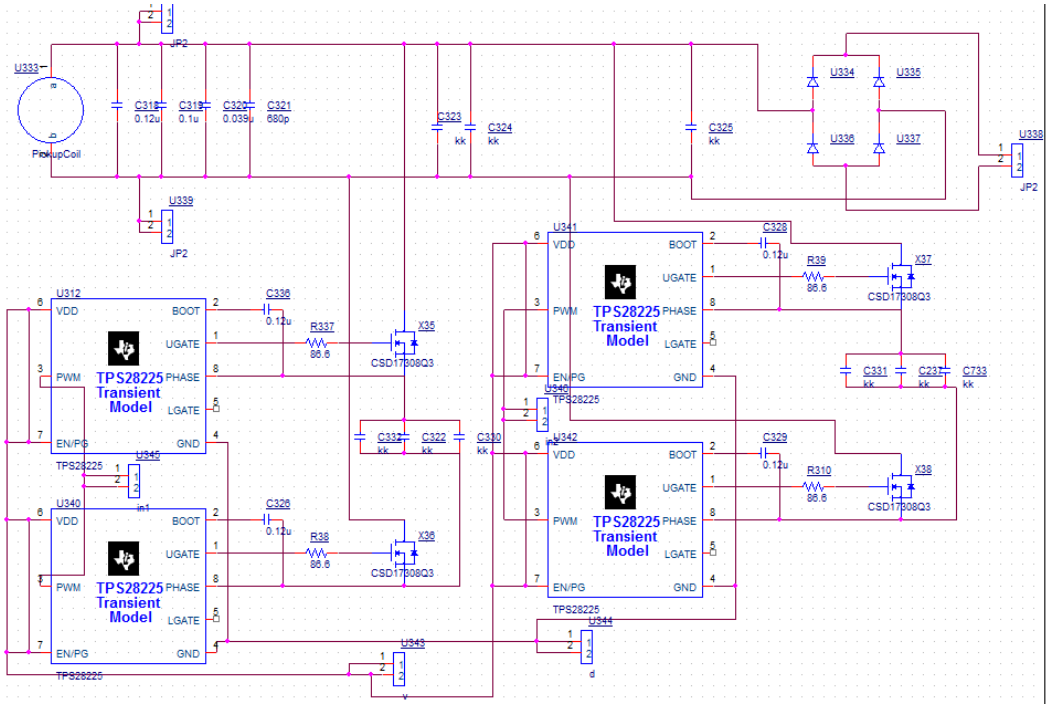

Figure 4-11 pick-up circuit with active capacitors tank

4.3.2 PCB Layout for Pick-up Circuit and Power Converter

PCB is designed according to [http://www.ti.com/lit/an/snva054c/snva054c.pdf].

1 PCB of the transmitter control signal circuit 1:

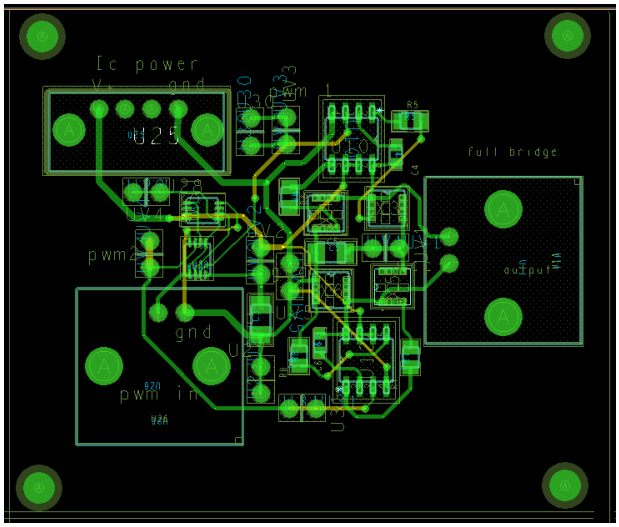

Figure 4-12 transmitter control signal circuit 1PCB layout

Circuit 2 (with the delay IC):

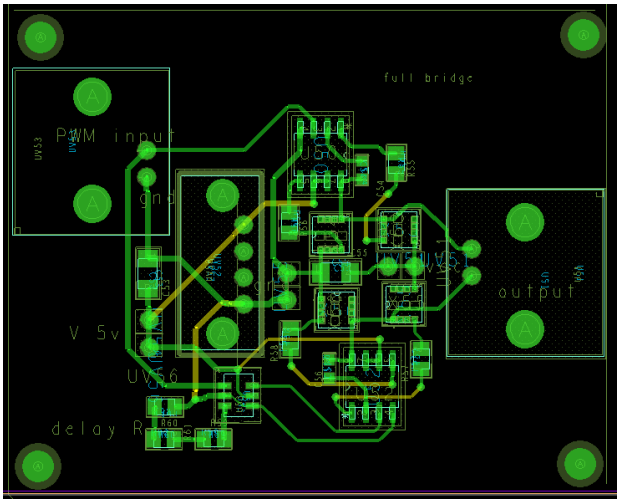

Figure 4-13 transmitter control signal circuit using delay IC PCB layout

3 Transmitter compensation circuit:

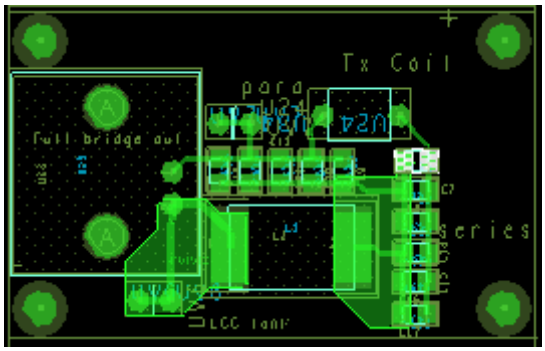

Figure 4-14 Transmitter compensation circuit PCB layout

4 Receiver pick-up circuit:

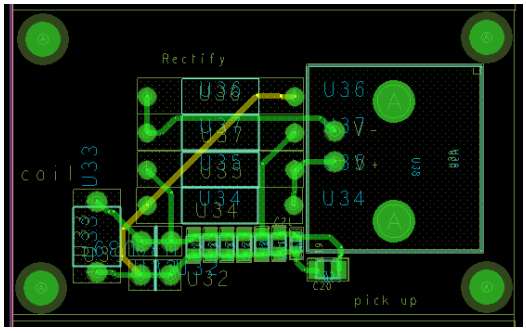

Figure 4-15 Pick-up compensation and rectifier circuit PCB layout

Receiver pick-up circuit with active capacitor tank:

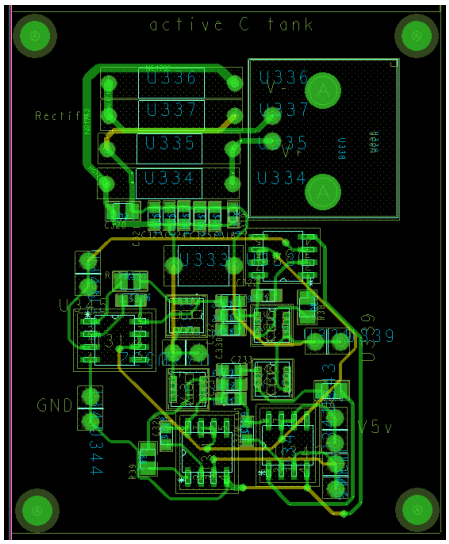

Figure 4-16 Receiver pick-up circuit with active capacitor tank PCB layout

4 Tri-state-boost converter (without digital isolator IC):

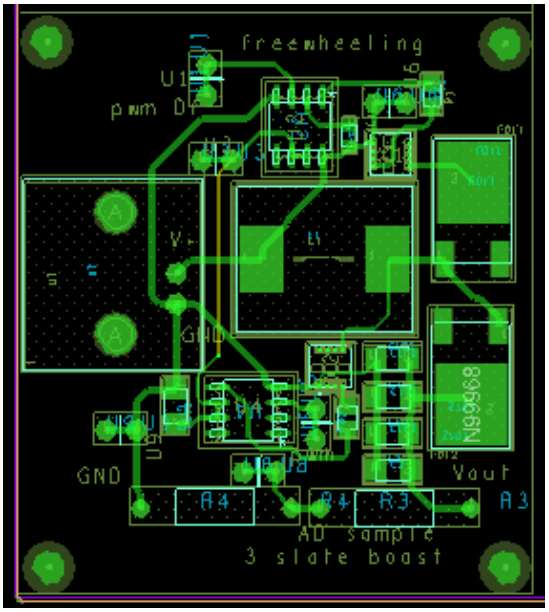

Figure 4-17 tri-state-boost converter PCB layout

4.4 Controller Design

4.4.1 Overall control

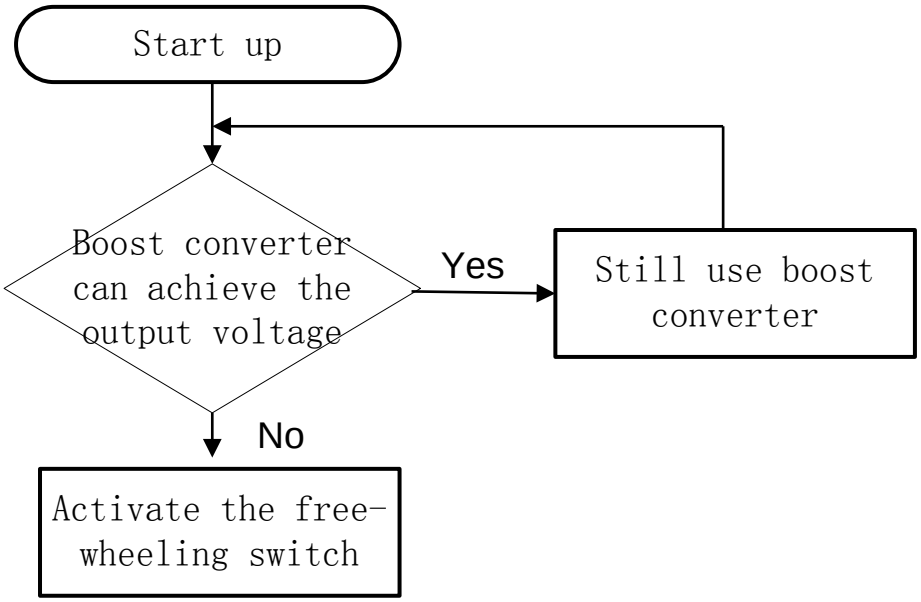

Figure 4-18 Overall control

When the output voltage can reach the expected value, the system uses the hysteresis boost control to regulate receiver output voltage

When the boost switch is saturated (the boost switch S_b always off, and the output voltage still can't reach the output level, then system is detuned", freewheeling switch will then activated.

4.4.2 TMS320F28335 Controller

Overall the system control is achieved by the Texas Instrument C2000 series MCU TMS320F28335. Program code is written in C language. However, the input frequency is 100Khz, so this requires that the switching frequency of S_f is at lease 200Khz synchronized

to twice of the V_{ac} frequency after the rectifier. The switching frequency of switch S_b which is used to control the output voltage is between 1Khz to 20Khz which requires that the feedback voltage sampling frequency should be much higher than that. TI C2000 series MCU has 150Mhz system frequency, ideally it can finish all the high frequency tasks easily. Although the floating point unit can help the MCU finish the calculation task very quickly, however it is not perfectly good to control the system in very high frequency and this is be discussed in the following parts.

Overall Structure:

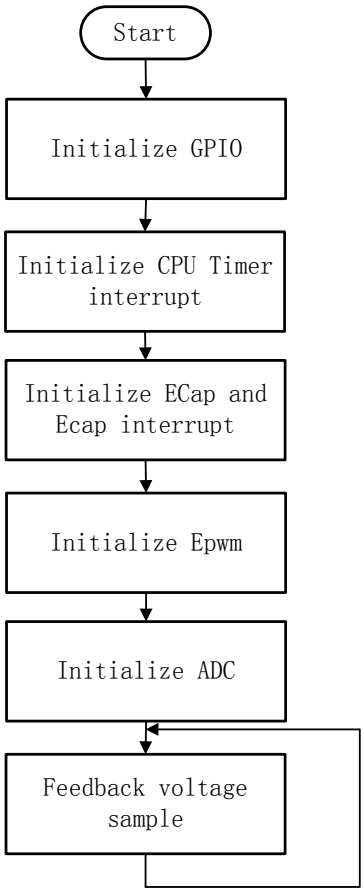

Figure 4-19 main function flow chart

4.4.3 Voltage Sense and Control

TMS320F28335 has 12bit Analog-to-Digital module which can be used to get the feedback voltage. Feedback voltage is the output voltage with resister voltage divider: $V_{fb} = \frac{R_1}{R_1+R_2} \times V_{out}$. The expected value of V_{out} is 5V, R_1 is 18Ω and R_2 is 33Ω like shown in Figure 4-5 voltage divider feed-back for TMS320F28335 ADC module. Register for ADC in

TMS320F28335 is a 16bits register, with lowest 4 bits not used. Normally the result of ADC is $\mathrm{ADC_{result}} = (\mathrm{Volt_{input}} - \mathrm{ADC_{L0}}) \times \frac{65520}{3.0}$, where $\mathrm{Volt_{input}}$ is the input voltage and $\mathrm{ADC_{L0}}$ is the analog voltage reference zero. $\mathrm{ADC_{L0}}$ is connected to the ground level to the MCU board. Input voltage is between 0 volt and 3 volt according to TI Controlsuite [9]. Ideally the ADC module with 12bits resolution is very precise, but according to practical experience, the resolution is about 9 bits during the hands on using. In this project, the nonlinearity and drift of reference zero problems are not considered. For a 4.25V to 4.45V hysteresis band, the corresponding $\mathrm{ADC_{result}}$ are 32760 and 34301.

CPU Timer1 is used for the output voltage control sampling. During the CPU Timer1 interrupt, the controller needs to detect if the feedback voltage is within the hysteresis band. If the ADC Digital Result as defined in last few paragraph is over 34301, set output pin GPIO4 high; if the result is smaller than 32760, set the output pin low. This sampling frequency 100Khz sampling rate which is much higher than the boost switch control frequency about 1Khz to 20Khz.

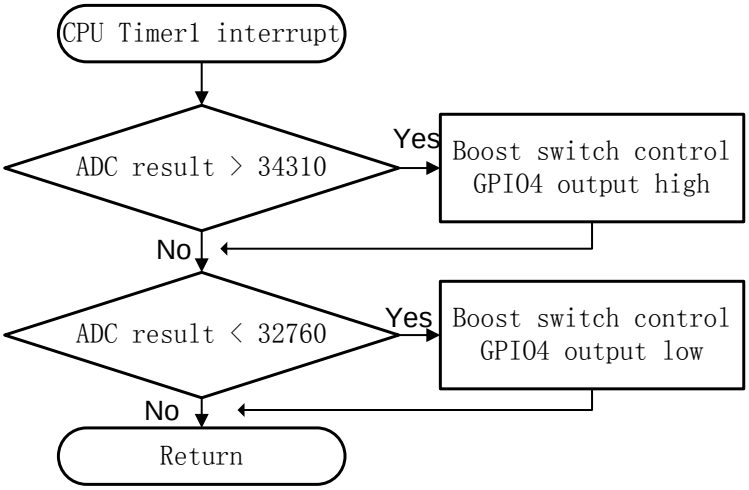

Figure 4-20 CPU Timer1 interrupt flow chart

4.4.4 Freewheeling Duty Cycle Calculation and Synchronization

Firstly, the result of V_{ac} and V_{oc} detection circuit using Op-amp and positive And gate are two pulse waveforms into the TMS320F28335 input pins. Cpu timer0 is used to read if those two input are high or low in 1.25Mhz. If the input is high then set a corresponding register as 1 and register -1 if input is low. Here Prdct is a defined 16-bit signed variable for the multiplying result of the two register values. And ‘add’ is a defined 16-bit signed variable for 20times the Prdct’s integration results. This is to achieve the integration in digital controller.

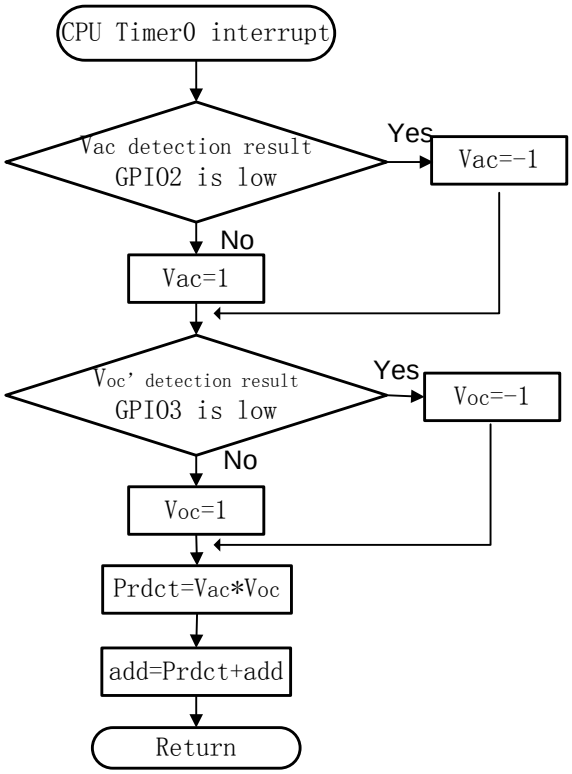

Figure 4-21 CPU Timer0 interrupt flow chart

TMS320F28335 chip has 6 Enhanced Capture modules which can be used to measure exterior pulse width precisely. For each module, it can capture the time of exterior pulse rising edge and falling edge. So it is very suitable to use the Ecap module to catch the rising edge time of V_{ac} detection results and measure the pulse period. The module can be initialized to be triggered by the rising up edge and set that time as the starting time. When the rising up edge of the second period comes, the resulting time counting number will be saved in a corresponding register and trigger an Ecap interrupt. After the interrupt, the counter of the Ecap module is cleared to 0 and restart to increase in the new period again.

In Ecap interrupt, the code running time should not be too long, or it will affect the next capture time. Control signal of free-wheeling switch S_f is calculated and generated within this Ecap interrupt.

First thing in the interrupt is to get the integration result ‘add’ saved in another variable and set the ‘add’ to zero.

Sampling rate of the detection results is at 1.25Mhz which is much high than the D_f control signal frequency 200Khz.

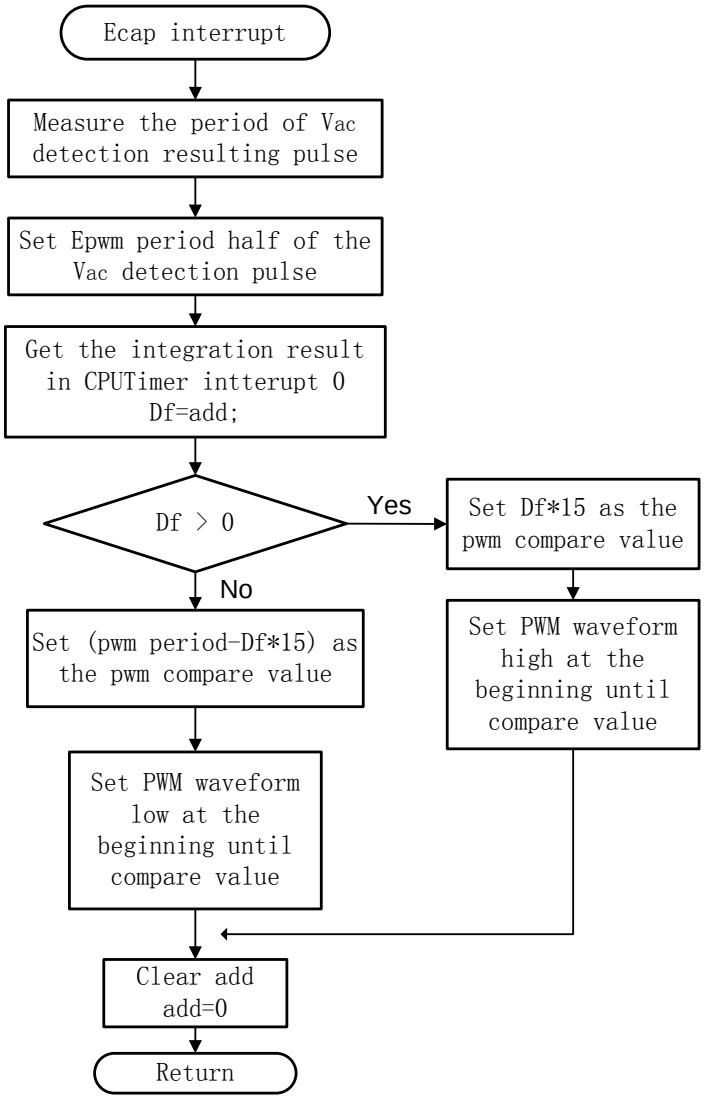

Figure 4-22 ECap interrupt flow chart

Secondly, an Enhanced Pulse Width Modulation module of TMS320F28335 is used here to generate the control signal. Set the period of the pwm signal exactly the half of the captured period. (make sure that the Epwm module and ECap module clock is the same) Then the

most important step comes. Controller needs to detect if the ‘add’ result is positive or negative to set the Epwm module. With a positive value, the generated pulse starts high at the ‘add’ part time. And when negative, ‘add’ will make the corresponding logic high at the end of each pwm period.

5 Chapter 5 Experimental Results

5.1 Transmitter

The hardware set of the transmitter coil, compensation circuit and control signal circuits is shown in the Figure 5-1 Transmitter hardware below.

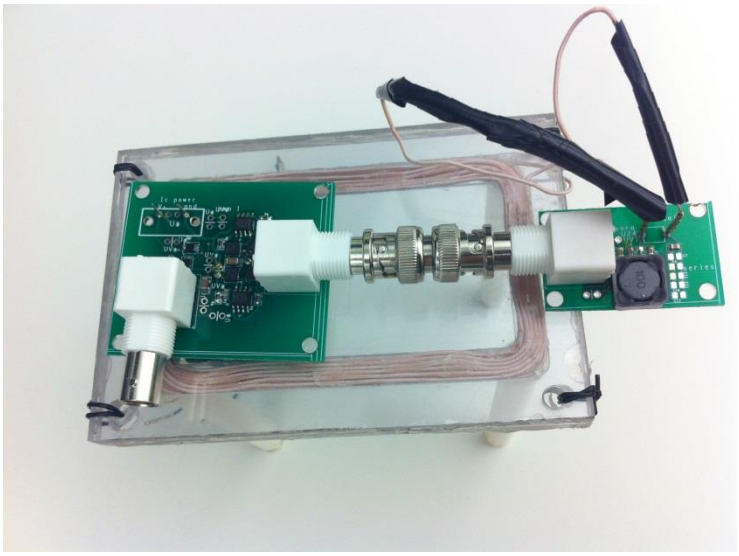

Figure 5-1 Transmitter hardware

1 Transmitter current and voltage under 5V, 100Khz, 80% duty cycle voltage input

Current waveform:

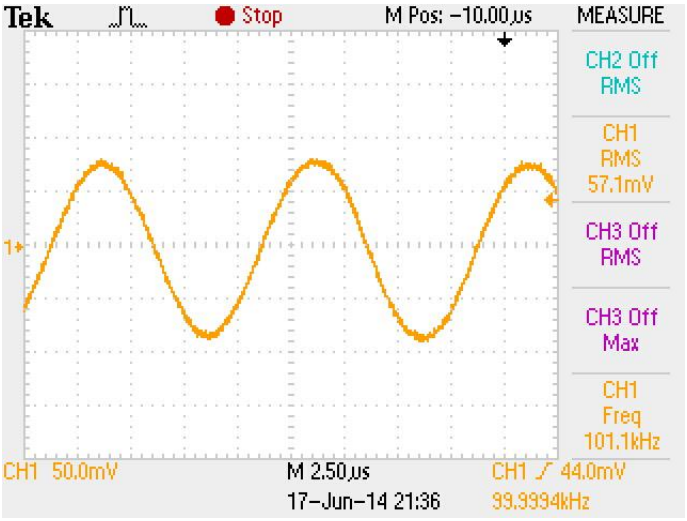

Figure 5-2 Transmitter coil current waveform, 100mV/1A

2 Transmitter voltage waveform:

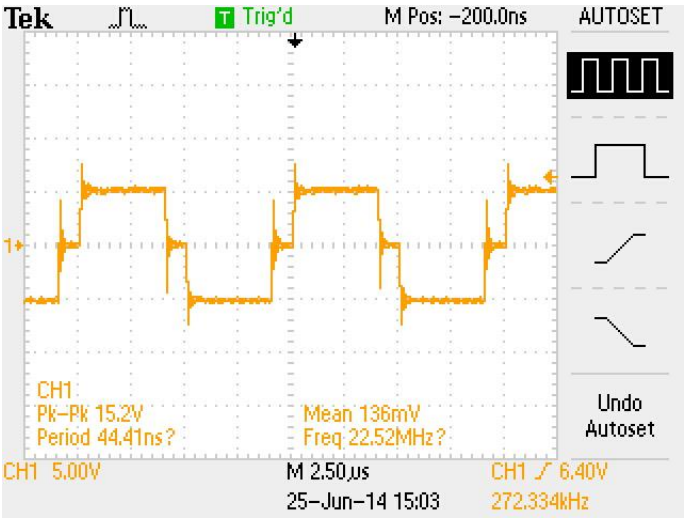

Figure 5-3 inverter voltage output waveform

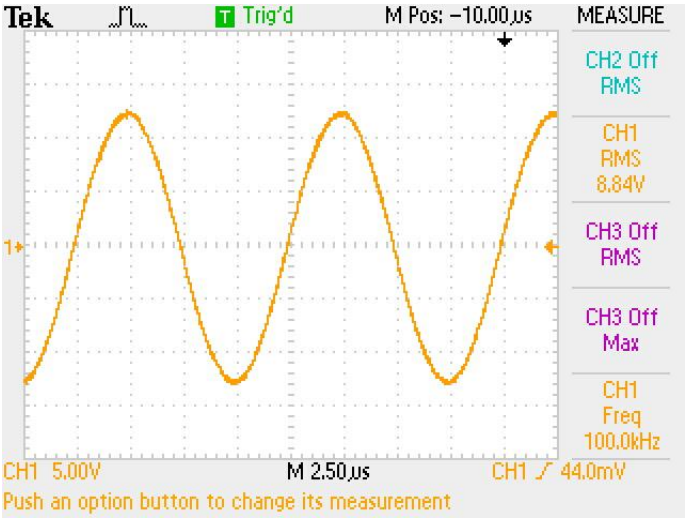

Figure 5-4 Transmitter coil voltage waveform

From the above hardware result, the RMS value corresponding maximum value is similar to the simulation results both in Simulink and PSpice.

5.2 Receiver side

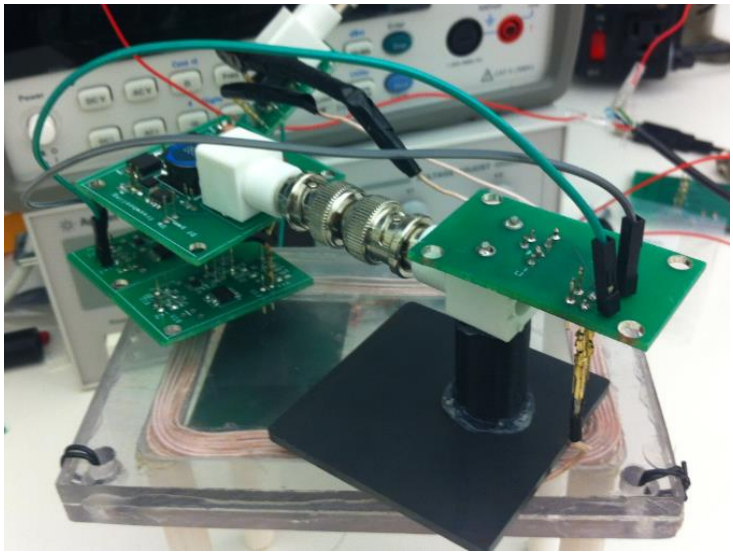

Figure 5-5 Receiver

5.2.1 $\mathbf{V_{oc}}$ waveform:

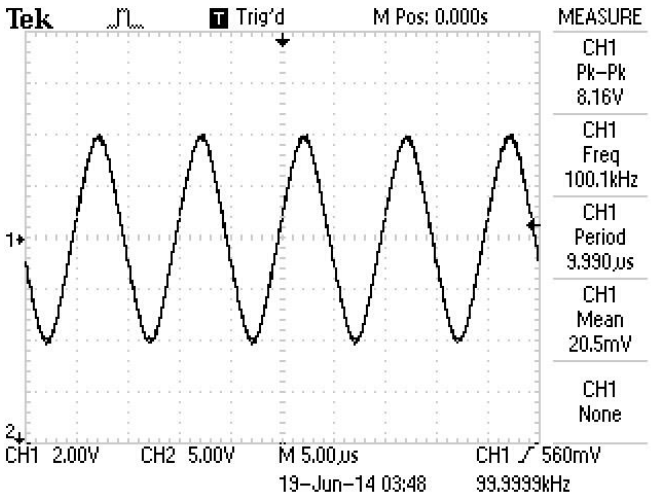

Figure 5-6 Receiver coil open circuit voltage V_{oc} waveform

5.2.2 Boost converter performance:

V_{out} receiver at slightly detuned condition (detuning factor $\frac{1}{3}$, Receiver compensation capacitor is chosen not to be the tuning value. Output voltage control hysteresis band is 4.25V to 4.45V. Discussion of the hysteresis band and output voltage resolution is at the end of the section.

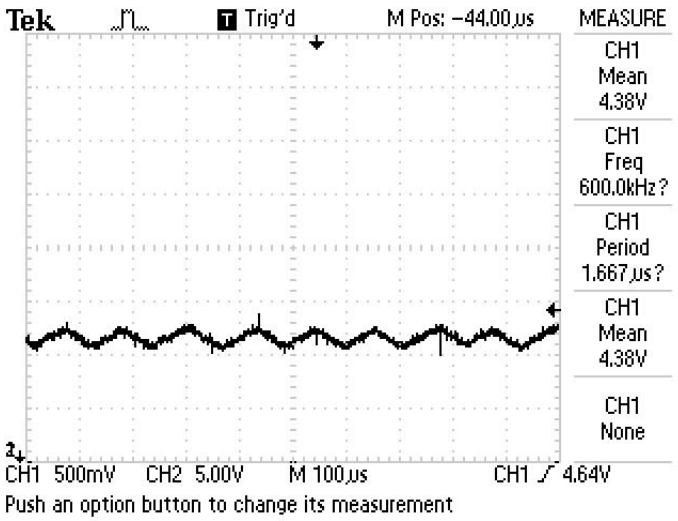

Figure 5-7 Boost converter receiver output voltage waveform

Figure 5-7 Boost converter receiver output voltage waveformshows that the result voltage is the expected value with switching frequency at about 8Khz. Boost converter can still have the output power in slightly detuned condition.

When receiver is highly detuned with a 160 nF parallel compensation capacitor:

V_{out} waveform is:

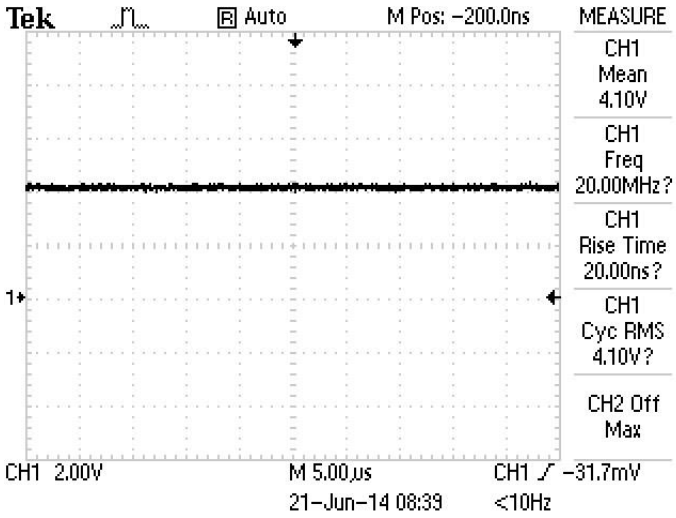

Figure 5-8 seriously detuned boost converter receiver output voltage

With a wider hysteresis band for the output voltage (4.39V to5.02V, corresponding ADC value is 33910 and 38687), the output voltage of the boost converter waveform is:

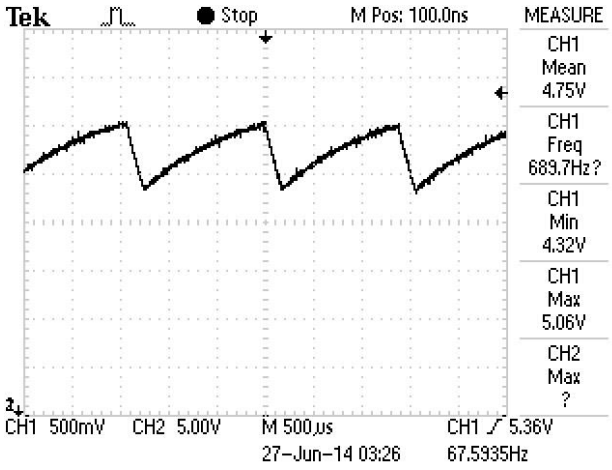

Figure 5-9 output voltage of the boost converter waveform with 4.39V to 5.02V hysteresis band

The actual ripple is a little bigger than the hysteresis band set in the MCU program. The min and max output voltage value of the hardware set up are 4.32V and 5.06V. The possible reasons for this are perhaps the zero drift of the MCU ADC that causes the ADC not getting very exact feedback voltage, or perhaps the load resisters not very accurate 18Ω and 33Ω that the feedback voltage resister dividers don't have precise voltage value for the ADC.

5.2.3 Tri-state boost converter

1 Instead of using tri-state-boost converter at the receiver side, a 1.95V DC voltage input is given to show if the converter can work normally at first step. Figure 5-11 the votlage waveform of point A in figure 5.8shows the point A voltage.

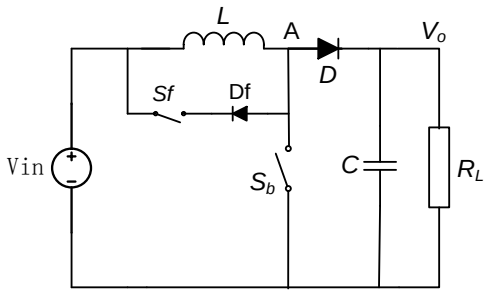

Figure 5-10 Tri-state-boost converter with DC voltage input

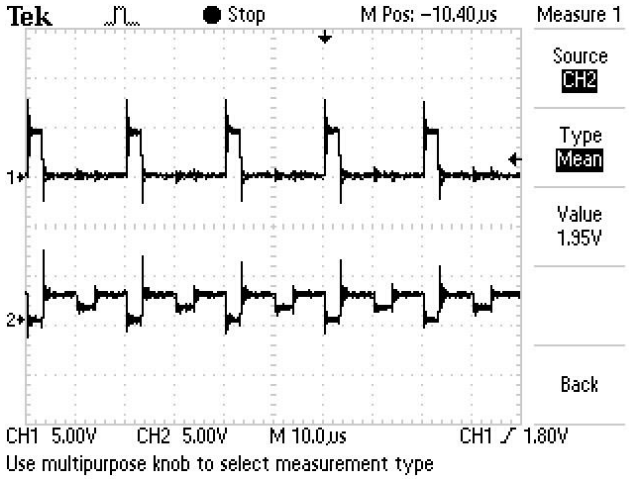

Figure 5-11 the votlage waveform of point A in figure 5.8

From Figure 5-11 the votlage waveform of point A in figure 5.8, it is clear that the tri-state-boost works. 20% D_f and 20% D_b are given to the converter. When S_b is on, voltage of A is short circuited to the ground. When S_f is on, voltage of A is shor circuited to the input

voltage. Output voltage is 2.6V，the hardware result is low than that voltage because of the open loop voltage control.

Digital isolator:

Digital isolator chip sends the control signal to driver IC TPS28225. The gate driver output to the MOSFET waveform is shown in Figure 5-12 Gate voltage of the free-wheeling switch signal waveform to ground.

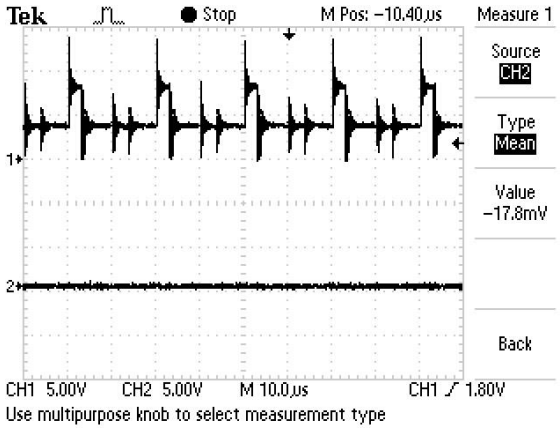

Figure 5-12 Gate voltage of the free-wheeling switch signal waveform to ground

From the Figure 5-12 Gate voltage of the free-wheeling switch signal waveform to ground, gate voltage of free-wheeling switch is seriously affected by the boost switch. But even when the free-wheeling S_f somehow opens by the effect of switch S_b, leaving the two switches both on at the same time, current will still only flow through S_b because of the diode. So the voltage spike caused by S_b won't cause big problems.

2 Detection circuit result

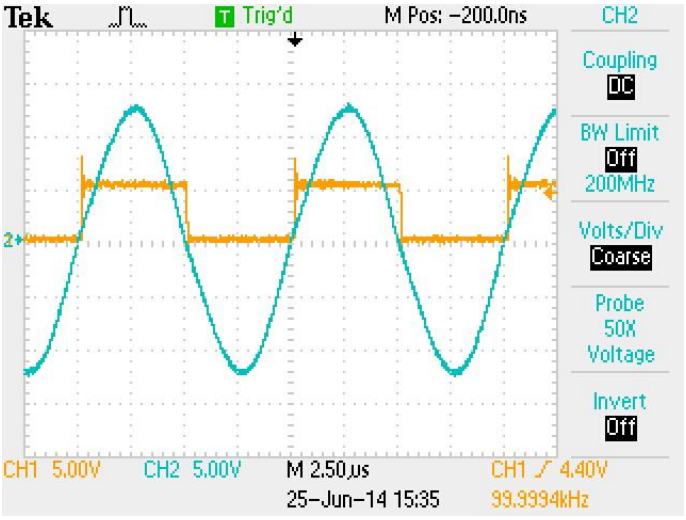

Figure 5-13 V_{ac} detection circuit results (blue line is V_{ac}, orange line is the result)

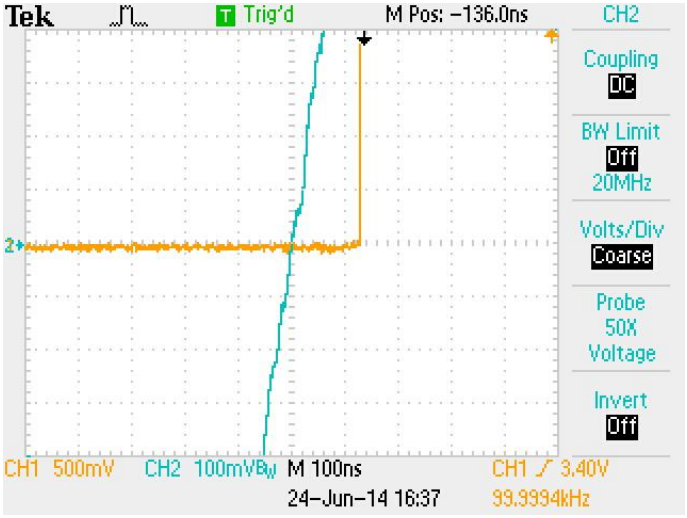

Figure 5-14 zoom-in of the figure 5-12

Take the V_{ac} detection circuit for example, the detection circuit performance is shown in Figure 5-13 V_{ac} detection circuit results (blue line is V_{ac}, orange line is the result). Figure 5-14 zoom-in of the figure 5-12 that the resulting waveform is about 120ns delay than the input waveform, possibly caused by the Op-amp IC or by the 'AND' gate IC in the detection circuit. The output of the Op-amp is an analog waveform for the 'AND' gate digital IC input, that will also have some influence. Software compensation could be used here, however the code delay running in the interrupt program will produce some influence to the control, sometimes the program crashes.

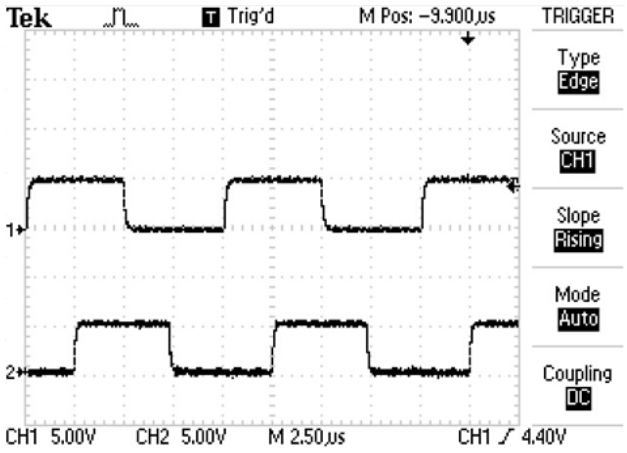

Figure 5-15 V'_{oc} and V_{ac} polarity detection circuit output waveform (channel 1 V'_{oc}, and channel 2 V_{ac})

Figure 5-15 V'_{oc} and V_{ac} polarity detection circuit output waveform (channel 1 V'_{oc}, and channel 2 V_{ac})shows the detection resulting pulse wave when circuit is tuned. The result is not the output of the detection circuit, but with 800Ω series resisters to limit the maximum

current to the Digital Controller. So the Figure 5-15 V'_{oc} and V_{ac} polarity detection circuit output waveform (channel 1 V'_{oc}, and channel 2 V_{ac})is actually slightly affected by the filter effect.

4 V_{oc} sense coil pick-up voltage V'_{oc}:

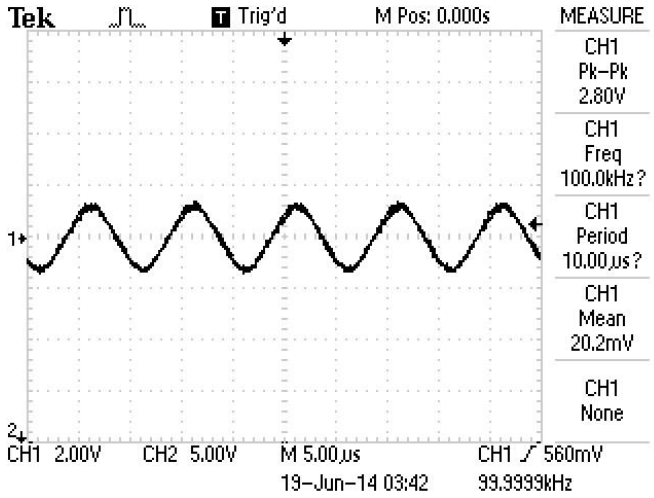

Figure 5-16 V_{oc} sense coil open circuit voltage V'_{oc} waveform

When free-wheeling control signal D_f is not connected to the circuit, the integration result is negative because of the capacitive resonant tank. D_f should be put at the end of each half V_{ac} cycle in 200Khz frequency. The resulting D_f signal with V_{ac} waveform is shown in Figure 5-17 Resulting D_f signal with V_{ac} detection waveform when control signal D_f is not connected to the circuit(channel 1 V_{ac} without the 800Ω current limit resister and channel 2 the D_f):

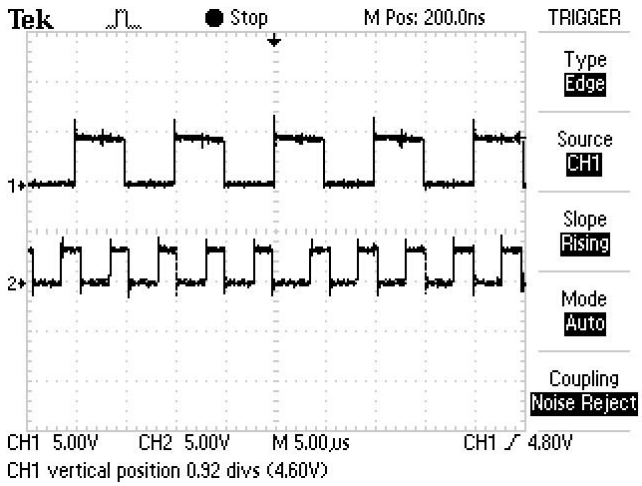

Figure 5-17 Resulting D_f signal with V_{ac} detection waveform when control signal D_f is not connected to the circuit

The resulting output voltage of the tri-state-boost is shown in Figure 5-20 output voltage waveform of tri-state-boost converter receiver.

Detection result of V_{ac} and V'_{oc} in same plot when D_f control signal is connected to the free-wheeling switch:

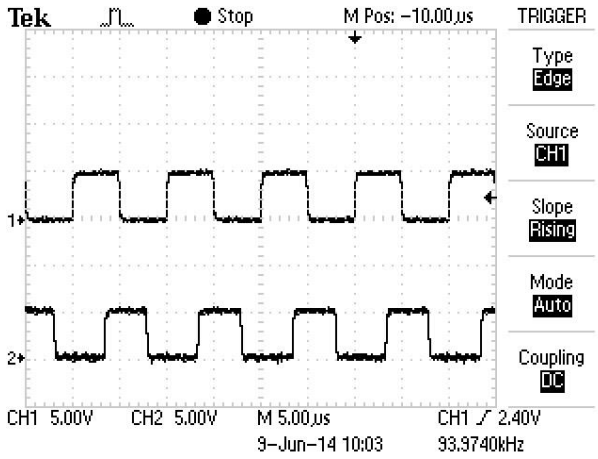

Figure 5-18 V'_{oc} and V_{ac} waveform of tri-state-boost converter receiver

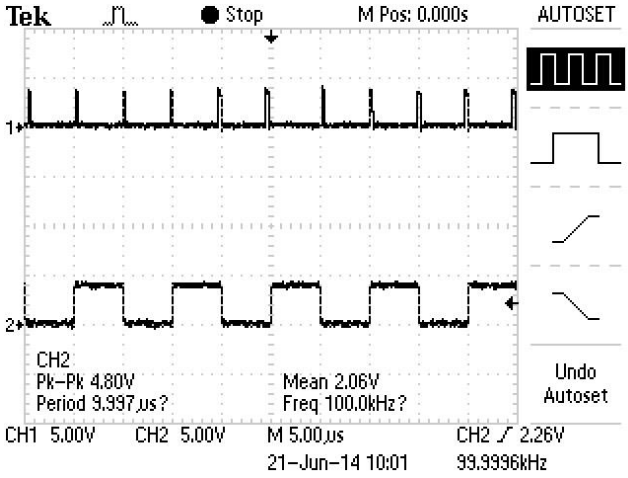

Figure 5-19 D_f signal with V_{ac} detection waveform

Figure 5-19 D_f signal with V_{ac} detection waveformshows that the resulting free-wheeling control signal is overall close to zero, and sometimes at the beginning of each V_{ac} half period sometimes at the end of each V_{ac} half period.

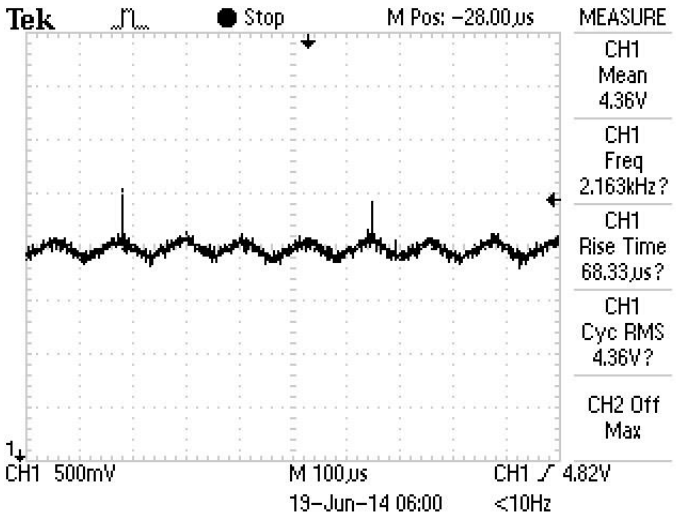

Figure 5-20 output voltage waveform of tri-state-boost converter receiver

Figure 5-20 output voltage waveform of tri-state-boost converter receiver shows the tri-state-boost receiver output voltage with a 160nF parallel compensation capacitor case.(hysteresis band is 4.25V to 4.45V)

6 Chapter 6 Conclusion and Summary

In this thesis, an Inductive Power Transfer system is built, simulated and implemented with both the transmitter and receiver.

The contributions of this thesis are summarized as follows:

- A low power scale IPT system is built with a constant receiver load and adjustable output voltage.
- Receiver active tuning strategy is simulated and implemented.
- Voltage mode hysteresis control is used because of the system robustness of the control.

Future research: although the active tuning of this low power scale IPT system is developed, there is still a lot of other work for further development of the IPT system. For example: active capacitor tank can be used in the pick-up circuit to make the system tuning more stable. An indirect method to detect the V_{oc} phase can be developed to remove the using of the additional receiver side coil, which can increase the system efficiency by decreasing the leakage flux.

References

[1] Pantic, Zeljko. Inductive Power Transfer Systems for Charging of Electric Vehicles. North Carolina State University, 2013.

[2] Pantic, Zeljko, Sanzhong Bai, and Srdjan M. Lukic. "Inductively coupled power transfer for continuously powered electric vehicles." Vehicle Power and Propulsion Conference, 2009. VPPC'09. IEEE. IEEE, 2009..

[3] Tri-State-Boost-Based Pickup Topology for Inductive Power Transfer

[4] Pantic, Zeljko, and Srdjan M. Lukic. "Framework and topology for active tuning of parallel compensated receivers in power transfer systems." Power Electronics, IEEE Transactions on 27.11 (2012): 4503-4513.

[5] Pantic, Zeljko, Sanzhong Bai, and Srdjan Lukic. "ZCS-Compensated Resonant Inverter for Inductive-Power-Transfer Application." Industrial Electronics, IEEE Transactions on 58.8 (2011): 3500-3510.

[6] Pickelsimer, Michael Christopher. "Wireless Power Transfer System with Power Factor Correction for Electric Vehicles." (2012).

[7] Boys, John T., Grant A. Covic, and Yongxiang Xu. "DC analysis technique for inductive power transfer pick-ups." Power Electronics Letters, IEEE 1.2 (2003): 51-53.

[8] Veerachary, Mummadi. "Signal flow graph modelling of multi-state boost DC–DC converters." IEE Proceedings-Electric Power Applications 151.5 (2004): 583-589.

[9] Switching Flow-Graph Nonlinear Modeling Technique Keyue Smedley, Member, IEEE, and Slobodan Cuk, Member, IEEE

[10] Bryant, James “Using Op Amps as Comparators” 2006 AN-849 at ww.analog.com/AN-849

[11] Si, Ping, et al. "Switching frequency analysis of dynamically detuned ICPT power pick-ups." Power System Technology, 2006. PowerCon 2006. International Conference on. IEEE, 2006.

[12] http://www.ti.com/controlsuite

[13] Si, Ping, and Aiguo Patrick Hu. "Analyses of DC inductance used in ICPT power pick-ups for maximum power transfer." Transmission and Distribution Conference and Exhibition: Asia and Pacific, 2005 IEEE/PES. IEEE, 2005.

[14] Dai, Xin, Yang Zou, and Yue Sun. "Uncertainty Modeling and Robust Control for LCL Resonant Inductive Power Transfer System." JOURNAL OF POWER ELECTRONICS 13.5 (2013): 814-828.

[15] Dietrich, Stefan, Ralf Wunderlich, and Stefan Heinen. "Stability considerations of hysteretic controlled DC-DC converters." Ph. D. Research in Microelectronics and Electronics (PRIME), 2012 8th Conference on. VDE, 2012.

[16] AN-1229 Simple Switcher PCB Layout Guidelines; Texas Instruments Incorporated, May 2004.

[17] N. Mohan, T.M. Undeland, and W.P. Robbins, “Power Electronics Converters, Applications and Design, New York: John Wiley & Sons., 3rd ef, pp.161-172, 2003